Discovery and in vitro and in vivo profiles of N-ethyl-N-[2-[3-(5-fluoro-2-pyridinyl)-1H-pyrazol-1-yl]ethyl]-2-(2H-1,2,3-triazol-2-yl)-benzamide as a novel class of dual orexin receptor antagonist

Ryo Suzuki [a], Dai Nozawa [a], Aya Futamura [a], Rie Nishikawa-Shimono [a], Masahito Abe [a], Nobutaka Hattori [a], Hiroshi Ohta [a], Yuko Araki [a], Daiji Kambe [b], Mari Ohmichi [c], Seiken Tokura [a], Takeshi Aoki [b], Norikazu Ohtake [a], Hiroshi Kawamoto [a,*]

[a] Chemistry Laboratories, Taisho Pharmaceutical Co., Ltd, 1-403 Yoshino-cho, Kita-ku, Saitama 331-9530, Japan
[b] Pharmacology Laboratories, Taisho Pharmaceutical Co., Ltd, 1-403 Yoshino-cho, Kita-ku, Saitama 331-9530, Japan
[c] Drug Safety and Pharmacokinetics Laboratories, Taisho Pharmaceutical Co., Ltd, 1-403 Yoshino-cho, Kita-ku, Saitama 331-9530, Japan

ABSTRACT

Orexins play an important role in sleep/wake regulation, and orexin receptor antagonists are a focus of novel therapy for the treatment of insomnia. We identified **27e** (TASP0428980) as a potent dual orexin receptor antagonist through the systematic modification of our original designed lead A. We demonstrated the potent sleep-promoting effects of **27e** at ip dose of 3 mg/kg in a rat polysomnogram study. **27e** exhibited relatively short half-life profiles in rats and dogs. Furthermore, accumulating evidence regarding ADME profiles indicates that the predicted human half-life of **27e** should be 1.2–1.4 h. These data indicated that **27e** has a short-acting hypnotic property, suggesting that **27e** might be useful for treating primary insomnia while exhibiting a low risk of next-day residual somnolence. Thus, **27e** and its related compounds should be further evaluated to enable advancement to clinical trials.

© 2015 Elsevier Ltd. All rights reserved.

1. Introduction

The orexin system is composed of two widely expressed G-protein-coupled receptors, orexin 1 (OX_1) receptor and orexin 2 (OX_2) receptor, and the two peptide agonists orexin A and orexin B (also known as hypocretin 1 and hypocretin 2), which are selectively expressed in a small cluster of neurons in the lateral hypothalamus.[1,2] The OX_1 receptor has a high affinity for orexin A, with its affinity for orexin B being 1 to 2 orders of magnitude lower, whereas the OX_2 receptor exhibits an equally high affinity for both peptides.[2] Both receptors are coupled to $G_{q/11}$ proteins and contribute to the activation of phospholipase C, leading to the elevation of intracellular Ca^{2+} concentrations.[2] The OX_2 receptor can also be coupled to the G_s and G_i pathways.[3] The orexin neurons and receptors are widely distributed in the brain, including the basal forebrain, limbic structures, and brainstem regions. The patterns of receptor expression partially overlap, but some regions express only one of the receptors. This pattern of expression suggests that the two types of receptors may have different physiological roles.[4]

The orexin system also has been implicated in numerous physiological functions, including feeding, addiction, depression, anxiety, panic, and lung/respiratory function, as suggested from animal studies.[4,5] A key role of the orexin system in the regulation of the sleep/wake cycle has been suggested by observations that mice lacking orexin peptides or both receptors display a strong narcoleptic-like phenotype with cataplexy[4] and that familial canine narcolepsy is caused by defective OX_2 receptor signaling.[6] Furthermore, the orexin levels in cerebrospinal fluid (CSF) vary during the circadian cycle in rodents, monkeys, dogs, and humans, with levels being highest at the end of the wake-active period and lowest toward the end of the sleep period.[7]

Positive allosteric modulators of $GABA_A$ receptors, such as zolpidem, are responsible for mediating the mechanism of action

involved in the current standard of care for insomnia. This mechanism is widely known to promote sleep through the suppression of CNS activity, which can be associated with serious adverse effects including muscular relaxation, memory disturbance, rebound insomnia, tolerance, and dependence. These concerns have encouraged further efforts to discover and develop treatments for insomnia with mechanisms of action that differ from those of current therapies. Novel treatments for insomnia have therefore targeted the orexin system, and the discovery of dual OX_1/OX_2 antagonist has been reported.[8,9] Positive clinical proof-of-concept (POC) studies have demonstrated sleep induction by four dual orexin receptor antagonists (DORAs): almorexant, SB-649868, suvorexant, and filorexant (MK-6096).[9] Importantly, these compounds have been shown to induce a physiological sleep architecture characterized by increases in the time spent in rapid eye movement (REM) and non-REM (NREM) sleep in animals and humans, differentiating them from $GABA_A$ modulators that reduce the time spent in these sleep stages, which are believed to be important for the consolidation of memory and the restorative functions of sleep. However, in Phase 2 and Phase 3 clinical trials, the most common adverse event associated with suvorexant, the most advanced DORA, was somnolence, with a dose-related increase in events observed across treatment groups.[10] The half-life of suvorexant in humans is 9–13 h, which is much longer than that of SB-649868 when analyzed clinically.[11] SB-649868 has been reported to have a half-life in the range of 3.4–3.9 h in healthy volunteers.[12] Furthermore, patients

with primary insomnia reported that SB-649868 significantly improved the quality of their sleep, while objectively increasing the total sleep time, reducing sleep latency, and suppressing nighttime awakenings.[14] The assessment of next-day residual effects indicated no significant differences between SB-649868 and placebo.[13,14] Thus, SB-649868 showed positive results in terms of efficacy, despite its short half-life profile, without inducing residual next-day effects.[12–14]

Therefore, we defined the discovery of a potent and short-acting DORA, compared with suvorexant, as a clear research goal. Here, we describe the characterization of N-ethyl-N-[2-[3-(5-fluoro-2-pyridinyl)-1H-pyrazol-1-yl]ethyl]-2-(2H-1,2,3-triazol-2-yl)-benzamide (**27e**, TASP0428980), a potent and structurally distinct DORA that is currently being evaluated in preclinical studies for primary insomnia (Fig. 1).

2. Chemistry

The routes of synthesis are summarized in Schemes 1–7. The pyrazole derivatives **4a–4f** were synthesized as described in Scheme 1. Commercially available 1-(tetrahydro-2H-pyran-2-yl)-5-(4,4,5,5-tetramethyl-1,3-dioxaborolan-2-yl)-1H-pyrazole (**1**) was transformed into **2a–2f** via Suzuki–Miyaura coupling with appropriate aryl bromides and the removal of the THP group in acceptable yields. N-Alkylation of **2a–2f** with 3-ethyl-1,2,3-oxathiazolidine 2,2-dioxide using sodium hydroxide as a base yielded **3a–3f**. Finally,
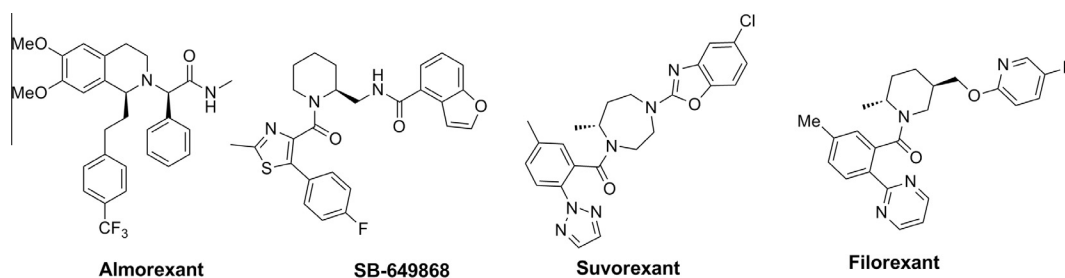

Figure 1. Representative dual OX_1 and OX_2 receptor antagonists.
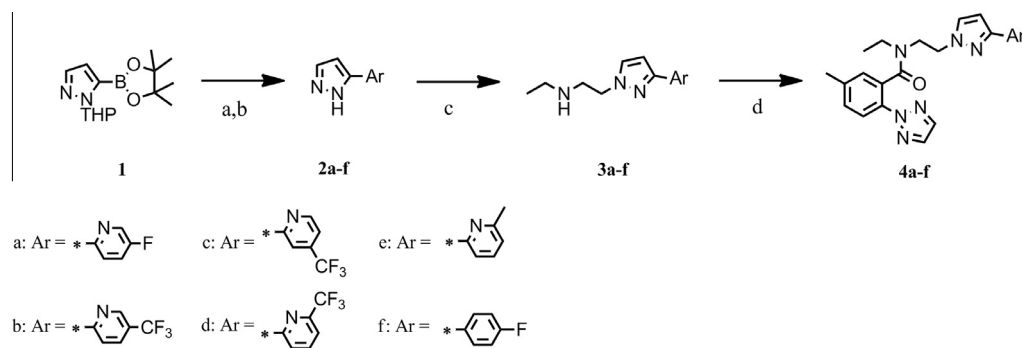
Scheme 1. Synthesis of pyrazole derivatives **4a–4f**. Reagents and conditions: (a) ArBr, Pd(PPh₃)₄, Na₂CO₃, H₂O, EtOH, toluene, 90 °C; (b) 4N HCl–AcOEt, MeOH, rt; (c) (1) 3-ethyl-1,2,3-oxathiazolidine 2,2-dioxide, NaOH, CH₃CN, 70 °C; (2) 25% H₂SO₄, 70 °C; (d) 5-methyl-2-(2H-1,2,3-triazol-2-yl)benzoic acid, T3P or WSC·HCl or HATU.
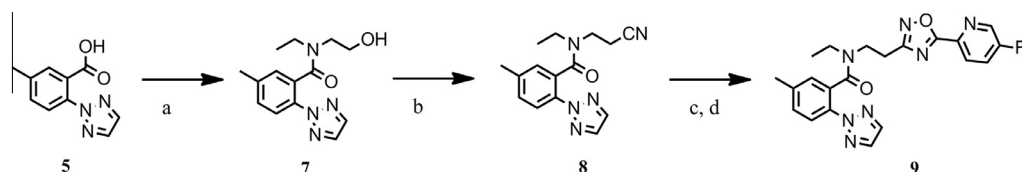
Scheme 2. Synthesis of oxadiazole derivative **9**. Reagents and conditions: (a) (1) SOCl₂, CHCl₃, reflux; (2) 6, TEA, CHCl₃, rt; (b) (1) MsCl, TEA, CHCl₃, rt; (2) NaCN, DMF, 80 °C; (c) 50% NH₂OH, EtOH, 80 °C; (d) (1) 5-fluoropicolinic acid, CDI, CH₃CN, DMF, rt; (2) DBU, 70 °C.
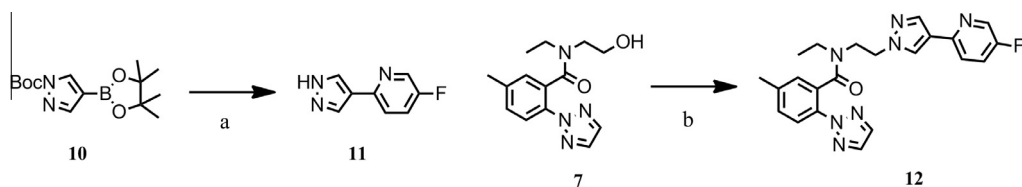
Scheme 3. Synthesis of pyrazole derivative **12**. Reagents and conditions: (a) 2-bromo-5-fluoropyridine, Pd(PPh₃)₄, Na₂CO₃, H₂O, EtOH, toluene, 90 °C; (b) (1) MsCl, TEA, CHCl₃, rt; (2) **11**, Cs₂CO₃, DMF, 80 °C.
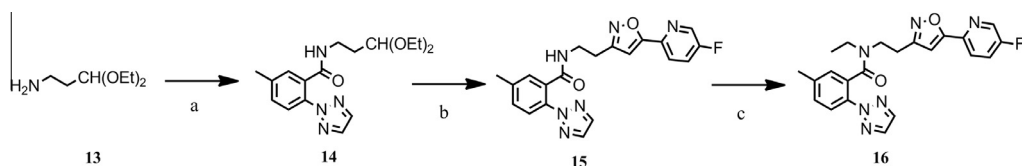
Scheme 4. Synthesis of oxazole derivative **16**. Reagents and conditions: (a) 5-methyl-2-(2H-1,2,3-triazol-2-yl)benzoic acid, HATU, DIPEA, DMF, rt; (b) (1) 1.2 M HClaq, THF, rt; (2) NH₂OH·HCl, AcONa, EtOH, H₂O, 0 °C; (3) NCS, DMF, rt; (4) 2-ethynyl-5-fluoropyridine, TEA, THF, rt; (c) EtI, NaH, DMF, rt.
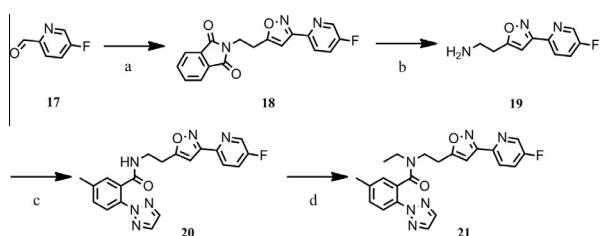

Scheme 5. Synthesis of isoxazole derivative **21**. Reagents and conditions: (a) (1) NH₂OH·HCl, AcONa, EtOH, H₂O, rt; (2) NCS, DMF, rt; (3) N-(3-butynyl)phthalimide, TEA, THF, rt; (b) H₂NNH₂·H₂O, EtOH, 90 °C; (c) 5-methyl-2-(2H-1,2,3-triazol-2-yl)benzoic acid, HATU, DIPEA, DMF, rt; (d) EtI, NaH, DMF, rt.

amide condensation of 5-methyl-2-(2H-1,2,3-triazol-2-yl)benzoic acid with **3a–3f** provided the pyrazole derivatives **4a–4f**.

The 1,2,4-oxadiazole derivative **9** was synthesized as described in Scheme 2. The amide condensation of 5-methyl-2-(2H-1,2,3-triazol-2-yl)benzoic acid **5** with 2-(ethylamino)ethanol **6** in the presence of N-[(dimethylamino)-1H-1,2,3-triazolo-[4,5-b]pyridin-1-ylmethylene]-N-methylmethanaminium hexafluorophosphate N-oxide (HATU) provided alcohol **7**. The mesylation of the hydroxyl group followed by cyanation yielded **8**. Finally, the addition reaction of **8** with hydroxylamine followed by O-acylation of amidoxime and cyclodehydration provided **9**.

Compound **12** was prepared as shown in Scheme 3. Commercially available *tert*-butyl 4-(4,4,5,5-tetramethyl-1,3-dioxaborolan-2-yl)-1H-pyrazole-1-carboxylate **10** was converted to the pyrazole **11** using the Suzuki–Miyaura coupling reaction. The Boc-group was removed in this reaction. The mesylation of

the hydroxyl group in intermediate **7** followed by the N-alkylation of pyrazole **11** using cesium carbonate yielded the desired compound **12**.

The steps for synthesizing isoxazole derivative **16** are depicted in Scheme 4. The amide condensation of 5-methyl-2-(2H-1,2,3-triazol-2-yl)benzoic acid with amine **13** in the presence of HATU yielded **14**. The removal of the acetal group of **14** followed by condensation with hydroxylamine, the chlorination of oxime, and isoxazole cyclization provided the desired compound **16**.

The condensation of commercially available 5-fluoropicolinaldehyde **17** and hydroxylamine followed by the chlorination of oxime and isoxazole cyclization yielded **18** (Scheme 5). The removal of the phthalimide group of **18** yielded **19**. The resulting amine **19** was reacted with 5-methyl-2-(2H-1,2,3-triazol-2-yl)benzoic acid to yield the intermediate **20**. N-Ethylation of intermediate **20** provided the final target **21**.

The N-alkylated amides (**26a**, **26b**) were prepared by the condensation of amine **24** with 5-methyl-2-(2H-1,2,3-triazol-2-yl)benzoic acid, followed by N-alkylation of the amide of intermediate **25**. Intermediate **24** was obtained in 2 steps from *tert*-butyl(2-bromoethyl)carbamate: first the N-alkylation of pyrazole **2a**, followed by removal of the Boc-group of **23** (Scheme 6).

To obtain the pyrazole derivatives (**27a–27e**, Scheme 7), amine **3a** was coupled with the appropriate benzoic acids. Intermediate **3a** was synthesized as described in Scheme 1.

3. Results and discussion

We have been pursuing potent dual OX₁ and OX₂ receptor antagonists in terms of their sleep-promoting effects with or with-
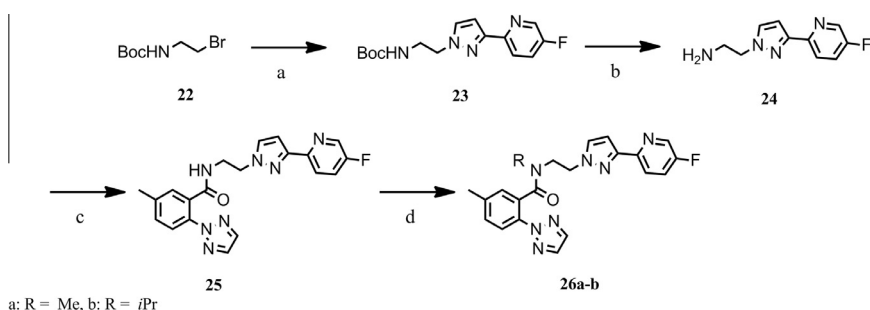
Scheme 6. Synthesis of N-alkyl derivatives **26a** and **26b**. Reagents and conditions: (a) **2a**, Cs₂CO₃, DMF, 80 °C; (b) 4 N HCl–EtOAc, EtOAc, rt; (c) 5-methyl-2-(2H-1,2,3-triazol-2-yl)benzoic acid, HATU, DIPEA, DMF, rt; (d) RI, NaH, DMF, rt.

Scheme 7. Synthesis of biarylamide derivative **27a–27e**. Reagents: (a) ArCO2H, WSC·HCl or T3P.

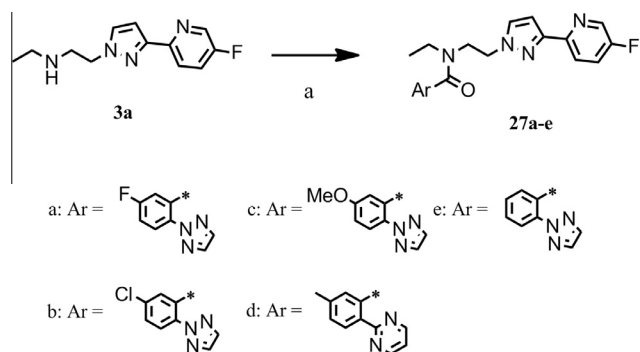out total sleep maintenance. Our strategy for designing lead compounds was to use a ligand-based drug design (LBDD) method, since several research groups have already reported various OX$_1$ and OX$_2$ receptor ligands. In addition, we adopted a hypothesis that a U-shaped conformation of *N,N*-disubstituted-1,4-diazepane **28** would elicit bioactivity through OX$_1$ and OX$_2$ receptors, since enforcing the U-shaped conformation by macrocyclization (**29a**)

resulted in a maintained or slightly improved antagonistic potency for the OX$_1$ and OX$_2$ receptors, compared with open compound **29b** (Fig. 2).[15]

We attempted to superimpose representative OX$_1$ and OX$_2$ receptor antagonists (suvorexant, filorexant and SB-674042) onto the quinazoline analogue **28** with the U-shaped conformation using the flexible alignment method of the Molecular Operating Environment program[16] with the default parameters and found that these molecules overlapped quite closely, as expected (Fig. 3). Based on this information, we created a novel pharmacophore model based on the superposition of these molecules, as shown in Figure 4. The pharmacophore model suggested that the cyclic amide linkages utilized coincidentally in the representative antagonists could be replaced with a linear amide linkage. As a result of the design of novel pharmacophore model and their fitting trials using the Ligand Pharmacophore Mapping protocol of the Discovery Studio program[17] with the default parameters, a pyrazolylethylbenzamide designed lead A was created as a linear linker. We decided to use designed lead A as a starting point for chemical modifications.

Our goals were to investigate the structure-activity relationship (SAR) of our novel lead class and to identify a potent dual OX$_1$ and OX$_2$ receptor antagonist in which the potency and pharmacokinetic profiles were appropriately balanced.
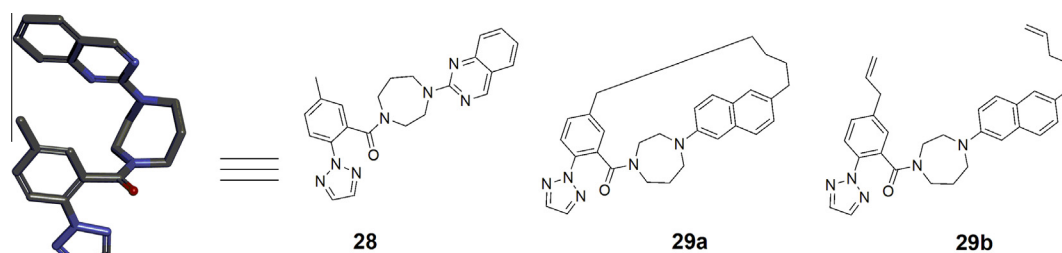

Figure 2. *N,N*-Disubstituted-1,4-diazepane derivatives **28** and **29**.
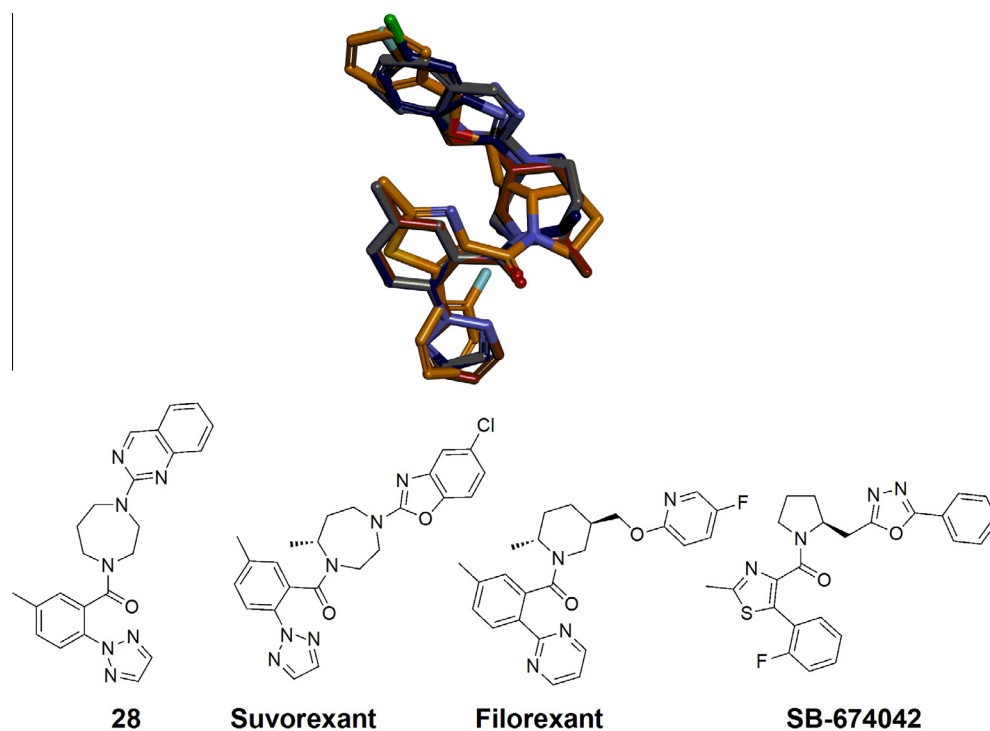

Figure 3. Superposition of compound **28** (gray), suvorexant (deep blue), filorexant (red) and SB-674042 (yellow).
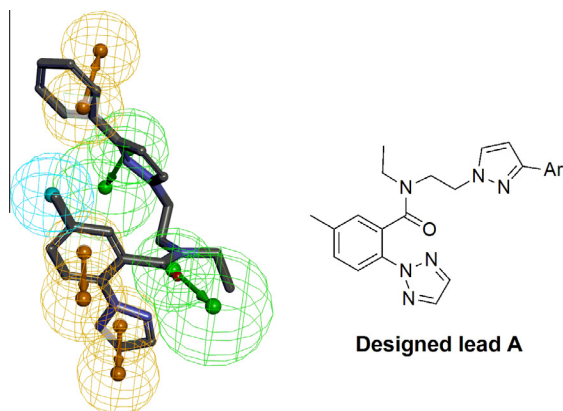
Figure 4. The pharmacophore model and the pyrazoylethylbenzamide designed lead A (Ar = phenyl). The pharmacophore model consists of two hydrogen bond acceptors (green arrows and spheres), one hydrophobic site (blue sphere), and three aromatic rings (orange arrows and spheres).

We initiated chemical modification to clarify the SAR in order from the aryl moiety at the right end of designed lead A. Table 1 highlights the SAR for the Ar part. First, the introduction of 5-fluoro-2-pyridine, which is used as a typical right-end component of known ligands such as filorexant, resulted in strong dual OX_1 and OX_2 receptor antagonistic activities. Various kinds of Ar replacements were then introduced with the exception of 2- and 4-fluoropyridine derivatives, since these analogues have a possibility of drug-protein covalent binding because of the potential electrophilicity of such fluoropyridine structures.[18] Among them, 2-trifluoromethyl-6-pyridine (**4d**), 6-methyl-2-pyridine (**4e**), and 4-fluorobenzene (**4f**) analogues showed almost the same antagonistic potency as that of **4a**. Unfortunately, these analogues had relatively high lipophilic natures. The $\log D/C\log P$ values tended to have limits between the values of 3 and 4.[19] Therefore, **4a**

Table 1
SAR of right-end Ar substituents

Compd	Ar	$K_b \pm SE^a$ (nM)		$C\log P^b$
		OX$_1$R	OX$_2$R	
4a		0.43 ± 0.04	0.89 ± 0.24	3.88
4b		48.57 ± 3.05	902.41 ± 144.99	4.68
4c		28.01 ± 3.58	66.43 ± 10.10	4.68
4d		3.19 ± 0.71	3.92 ± 2.04	4.68
4e		0.41 ± 0.04	1.96 ± 0.17	4.17
4f		0.32 ± 0.04	1.25 ± 0.36	5.02

[a] The K_b value is the mean of multiple results (at least three independent determinations performed in duplicate) with the standard error of the means.
[b] The $C\log P$ value was calculated using software from Daylight Chemical Information Systems, Inc.

Table 2
SAR of 5-membered heteroaromatics
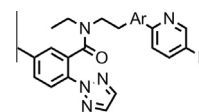
Compd	Ar	$K_b \pm SE^a$ (nM)		$C\log P^b$
		OX$_1$R	OX$_2$R	
4a		0.43 ± 0.04	0.89 ± 0.24	3.88
9		8.09 ± 1.64	22.99 ± 1.24	2.46
12		3.81 ± 0.62	7.22 ± 1.76	3.67
16		15.24 ± 4.32	19.78 ± 2.03	3.18
21		45.49 ± 2.93	32.19 ± 3.52	3.18

[a] The K_b value is the mean of multiple results (at least three independent determinations performed in duplicate) with the standard error of the means.
[b] The $C\log P$ value was calculated using software from Daylight Chemical Information Systems, Inc.

showing relatively low $C\log P$ value was used as a template for the following modifications. The $C\log P$ value was calculated using software from Daylight Chemical Information Systems, Inc.

Next, we attempted to find a novel and potent 5-membered heteroaromatic component. The replacement of the pyrazole with several kinds of ring systems, which could reduce their lipophilicity, was conducted as shown in Table 2. Oxadiazole analogue **9**, 1,4-pyrazole analogue **12**, and isoxazole analogues **16** and **21** showed moderate antagonistic activities for the OX_1 and OX_2 receptors. Only pyrazole analogues **4a** and **12** had potent dual OX_1 and OX_2 receptor antagonistic activities.

The effects of substituents at the amide nitrogen atom on intrinsic potency were investigated (Table 3). An amide NH proton analogue **25** dramatically decreased both the OX_1 and OX_2 receptor antagonistic activities. This effect might have been caused by the difficulty in forming a U-shaped conformation. The introduction of a methyl group (**26a**) at the amide nitrogen atom showed a single digit nano-molar potency against both OX_1 and OX_2 receptors. A more bulky substitution, such as an isopropyl group in **26b**, led

Table 3
SAR of N-alkyl substituents
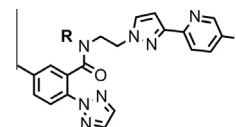
Compd	R	$K_b \pm SE^a$ (nM)	
		OX$_1$R	OX$_2$R
4a	Et	0.43 ± 0.04	0.89 ± 0.24
25	H	151.88 ± 35.05	376.10 ± 83.80
26a	Me	2.27 ± 0.10	8.58 ± 1.32
26b	iPr	38.46 ± 6.31	37.85 ± 3.91

[a] The K_b value is the mean of multiple results (at least three independent determinations performed in duplicate) with the standard error of the means.

Table 4
SAR of ethylpyrazole derivatives
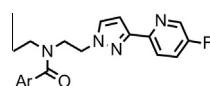
Compd	Ar	$K_b \pm SE^a$ (nM)		$C\log P^b$	hMS^c (%)
		OX$_1$R	OX$_2$R		
4a		0.43 ± 0.04	0.89 ± 0.24	3.88	35.0
27a		6.67 ± 0.44	11.42 ± 0.97	3.58	35.3
27b		1.48 ± 0.33	2.82 ± 0.19	4.15	46.9
27c		119.30 ± 41.58	638.10 ± 89.48	3.40	NT
27d		2.52 ± 0.22	4.01 ± 0.45	3.08	19.7
27e		5.00 ± 1.95	13.06 ± 5.58	3.38	24.1

[a] The K_b value is the mean of multiple results (at least three independent determinations performed in duplicate) with the standard error of the means.
[b] The $C\log P$ value was calculated using software from Daylight Chemical Information Systems, Inc.
[c] Metabolized percentage after 15 min of incubation in human liver microsomes (1 mg protein/mL, 5 μM).

Table 5
Pharmacokinetic profiles of **27d** and **27e** in rats and dogs

Compd	27d		27e	
	Rat	Dog	Rat	Dog
V_d (mL/kg)	1790	1290	1710	745
CL (mL/h/kg)	3910	786	3960	598
$T_{1/2}^*$ (h)	0.318	1.13	0.299	0.962
T_{max} (h)	0.667	0.500	0.833	0.667
F (%)	4.62	100	14.9	80.2
Brain/Plasma ratio	0.13	—	0.17	—
CSF/Plasma ratio	0.03	—	0.06	—
MS^a (%)	97.3	10.1	79.9	7.3

27d: For rats, intravenous administration at 2 mg/kg, oral administration (BA), or intraperitoneal administration (Brain/Plasma ratio and Cerebrospinal fluid/Plasma ratio) at 30 mg/kg to male rats. For dogs, intravenous administration at 0.5 mg/kg, and oral administration at 3 mg/kg to male dogs.
27e: For rats, intravenous administration at 2 mg/kg, and oral administration at 10 mg/kg to male rats. For dogs, intravenous administration at 0.5 mg/kg, and oral administration at 3 mg/kg to male dogs.
V_d, CL and $T_{1/2}$ were determined by intravenous administration. T_{max} was determined by oral administration. F (%) was comparison between intravenous administration and oral administration.
[a] MS (%): Metabolized percentage after 15 min of incubation in liver microsomes of rats or dogs (1 mg protein/mL, 5 μM).
[*] $T_{1/2}$: ln 2 * V_d/CL.

to a moderate potency. These results suggested that relatively small N-alkyl substituents were acceptable and that the ethyl group showing more potent intrinsic potency than the methyl group was an optimal N-alkyl substituent in terms of the OX$_1$ and OX$_2$ receptor antagonistic activities.

We optimized the three parts in **4a** as described above, and finally we undertook the optimization of the left end part, taking into account the bioavailability of the molecules in humans by assessing the in vitro stability in human microsomes. The replacement of the methyl group with fluoro, chloro, and methoxy groups

was conducted. Among them, the fluoro and chloro analogues **27a** and **27b** exhibited maintained orexin receptor antagonistic activities but did not show any improvements in metabolic stability. These results might have been due to their relatively high lipophilic natures. The methoxy group in **27c** played an important role in reducing the lipophilicity, while **27c** was not tolerated in terms of its OX$_1$ and OX$_2$ receptor antagonistic activities. On the other hand, alternative approaches to reducing lipophilicity worked to some extent. These approaches, including 1) the replacement of the triazole moiety in **4a** with a pyrimidine group (leading to
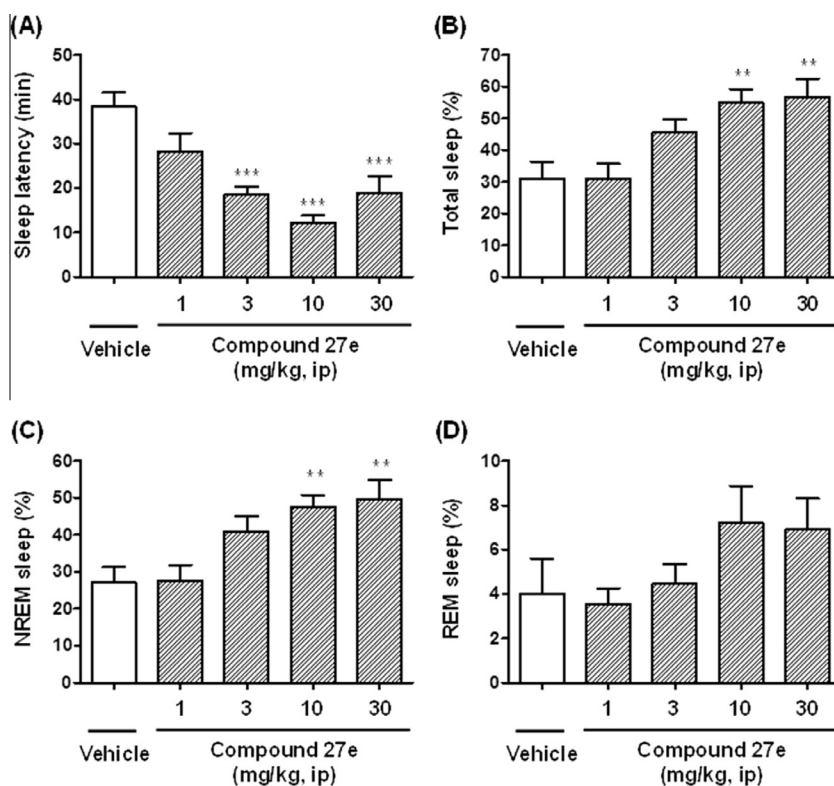
Figure 5. Effects of compound **27e** on sleep parameters in a rat polysomnography study. The sleep-promoting effects on the latency until the sleep stage (A), the percentage of time spent in total sleep (B), the time spent in non-REM (NREM) sleep (C), and the time spent in REM sleep (D) for the 2-h period after the intraperitoneal administration of the vehicle or compound **27e** are shown. Values are shown as the mean and SEM ($n = 8–10$ animals). $^{**}P <0.01$, $^{***}P <0.001$ versus vehicle-treated group, based on the Bartlett test followed by the Dunnett multiple comparison post-hoc test.
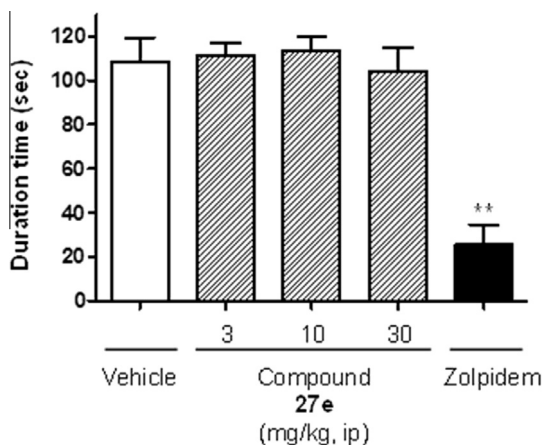

Figure 6. Effects of compound **27e** on rotarod performance test in rats. The compounds were administered 30 min prior to the test. $^{**}P <0.01$ versus vehicle-treated group (Steel test).
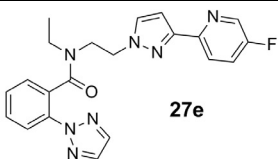
27d), and 2) the des-methylation of the tolyl moiety in **4a** (leading to **27e**), led to slight improvements not only in lipophilicity but also in microsomal stability while their OX$_1$ and OX$_2$ receptor antagonistic activities were tolerated.

All the compounds shown in Table 4, except for **27c**, had no significant difference. Accordingly, we thought that the lower lipophilic compounds would show smaller V_d values and, by extension, that these compounds might have relatively short half-life profiles. To confirm whether our strategy was correct, we selected the lowest lipophilic compounds **27d** and **27e**, and used them in rat and dog PK studies, even though these

compounds were not relatively potent. As expected, **27d** and **27e** exhibited relatively short half-life profiles, with a rapid T_{max} in rats and dogs. These compounds had poor bioavailability in rats (**27d**: 4.62%, **27e**: 14.9%) and good bioavailability in dogs (**27d**: 100%, **27e**: 80.2%). Compound **27e** was then evaluated in greater detail as a representative of *N*-pyrazolylethylbenzamide derivatives, since **27e** had a better CSF penetrability than **27d**. A major metabolite of **27e** was estimated to be the same in rat, dog, and human liver microsomes. Furthermore, the major elimination pathway was thought to be hepatic metabolism in rats, based on the low excretion rates of the parent compound **27e** in urine (0.4%) and bile (0.2%). The gastrointestinal absorption of **27e** seemed to be excellent, considering that it has moderate lipophilicity and acceptable aqueous solubility (30.2 μg/mL in pH6.8 phosphate buffer). Therefore, hepatic microsomal stability might be a good indicator of bioavailability. In fact, the hepatic microsomal stabilities data (%metabolized: rat: 79.9%, dog: 7.3%) agreed well with in vivo data demonstrating that **27e** has a low bioavailability in rats and a high bioavailability in dogs. Assuming that hepatic metabolism is the primary mode of elimination in vivo, **27e** was predicted to have good bioavailability in humans. Therefore, further in vivo evaluation of **27e** was conducted as a representative of *N*-pyrazolylethylbenzamide derivatives (Table 5).

The sleep-promoting effect of the most balanced compound, **27e**, was evaluated using a rat polysomnogram (PSG) study at an intraperitoneal (ip) dose of 1–30 mg/kg in consideration of its low oral bioavailability in rats. Freely moving rats with chronically implanted electrodes were well habituated to the experiment boxes and had access to food and water ad libitum. The compound **27e** or vehicle was administered prior to lights off (start of the active phase) and the start of recording. In the present study, **27e** showed a fast onset of action after dosing. The effects of **27e** at

Table 6
Profiles of **27e**

In vitro profiles[a]
Antagonistic activity[a]
hOX_1 ($K_b \pm SE$) 5.00 ± 1.95 nM
rOX_1 ($K_b \pm SE$) 5.08 ± 0.66 nM
hOX_2 ($K_b \pm SE$) 13.06 ± 5.58 nM
rOX_2 ($K_b \pm SE$) 6.06 ± 0.30 nM

Selectivity[d]
 92 items (receptor/transporter
binding or enzyme activity assays)
>50% at 10 μM: MT_3 (66%)

Physicochemical properties
solubility (pH6.8 PB) 30.2 μg/mL
ClogP 3.38

In vivo profiles
PK profiles

	rat	dog
V_d (mL/kg)[c]	1710	745
CL (mL/h/kg)[c]	3960	598
$T_{1/2}$ (h)[c]	0.299	0.962
T_{max} (h)[c]	0.833	0.667
F (%)[c]	14.9	80.2
Brain/Plasma[b]	0.17	
CSF/Plasma[b]	0.06	
Predicted human $T_{1/2}$ (h) sss method		
	1.2	1.4

Rat PSG MED 3.0 mg/kg ip
Rat rotarod performance model
                No Significant effect up to 30 mg/kg ip

[a] The K_b value is the mean of multiple results (at least three independent determinations performed in duplicate) with the standard error of the means.
[b] Brain/plasma and CSF/plasma of rats were collected at 0.5 h after drug administration (10 mg/kg, po) and the drug concentrations were measured (n = 3 rats/group).
[c] The pharmacokinetic study was conducted in fasted Sprague–Dawley rats (n = 3) and dogs dosed at 2 mg/kg and 0.5 mg/kg for intravenous dosing and dosed at 10 mg/kg and 3 mg/kg for oral dosing. V_d, CL and $T_{1/2}$ were determined by intravenous administration. T_{max} was determined by oral administration. F (%) was comparison between intravenous administration and oral administration. $T_{1/2}$ was calculated from ln 2 * V_d/CL equation.
[d] All the assays were performed at Cerep, France.

3–30 mg/kg showed a significant reduction in the latency until total sleep in a dose-dependent manner (C_{max} plasma levels: 728 nM at 3 mg/kg, ip, 0.33 h). Furthermore, the duration of NREM sleep was significantly increased at doses of 10 or 30 mg/kg, ip. The duration of REM sleep also tended to increase, but the difference was not significant during the 2-h period after administration. The current standards of care for insomnia, such as zolpidem (a $GABA_A$ receptor modulator), are well known to attenuate sleep latency and to promote NREM sleep, but they also suppress the REM components of normal sleep. Meanwhile, the sleep architecture induced by **27e**, a dual OX_1 and OX_2 receptor antagonist, is characterized by increases in both NREM and REM sleep (Fig. 5).

Furthermore, $GABA_A$ receptor modulator-induced sleep is also associated with a significant impairment of motor coordination. In the present study, compound **27e** at doses of 3, 10, and 30 mg/kg, ip, did not affect the rotarod performance of rats, while zolpidem at an oral dose of 10 mg/kg significantly impaired motor coordination (Fig. 6). These results suggest that compound **27e** is unlikely to impair motor coordination even when administered at a dose 10-fold above its effective dose in the PSG study. These results indicate that **27e** has potent sleep-promoting effects without inducing motor impairment.

Finally, we identified **27e** as a representative of *N*-pyrazolylethylbenzamide derivatives for further development. The detailed profiles of **27e** are summarized in Table 6. Compound **27e** showed potent OX_1 and OX_2 receptor dual antagonistic activities, and no species differences were observed between humans and rats (hOX_1: 5.00 nM, rOX_1: 5.08 nM, hOX_2: 13.06 nM, rOX_2: 6.06 nM). Compound **27e** was highly selective for orexin receptors when tested in 92 receptor/transporter binding or enzyme activity assays, including benzodiazepine, $GABA_A$, adenosine, melatonin and histamine receptors; it also exhibited acceptable solubility in aqueous media. We demonstrated potent sleep-promoting effects in a rat PSG study when **27e** was administered at 3 mg/kg, ip, without inducing motor impairment on the rat rotarod performance

test when administered at doses of up to 30 mg/kg, ip. Furthermore, **27e** showed acceptable DMPK profiles, good oral bioavailability in dogs (F = 80%) and moderate bioavailability in rats (F = 15%), good brain and CSF penetrability, and short half-life profiles with a rapid T_{max} in rats and dogs. The predicted human half-life (single-species scaling) was calculated to be 1.2–1.4 h.[20] Finally, **27e** was also predicted to have a rapid onset of action in humans. These data suggest that **27e** could be a useful drug for insomnia with a low risk of next-day drowsiness.

4. Conclusion

Our SAR characterization of a novel series of dual orexin receptor antagonist, represented by *N*-pyrazolylethylbenzamide derivatives, has led to the identification of **27e** as a potent, short half-life, brain-penetrating agent for the treatment of insomnia. The design of designed lead A was used as an LBDD method based on published DORAs. A reduced lipophilicity through systematic modification led to **27d** and **27e**, which exhibited acceptable liver microsomal stability and moderate lipophilicity profiles to obtain a relatively low V_d value compound. Finally, we identified *N*-ethyl-*N*-[2-[3-(5-fluoro-2-pyridinyl)-1*H*-pyrazol-1-yl]ethyl]-2-(2*H*-1,2,3-triazol-2-yl)-benzamide **27e** as an advanced compound. Compound **27e** had an excellent pharmacokinetic profile with a rapid T_{max} and a short half-life as well as good dual OX_1 and OX_2 receptor antagonistic activities. The compound also demonstrated potent sleep-promoting effects in a rat PSG study at a dose of 3 mg/kg, ip. Furthermore, the predicted human half-life (single-species allometric scaling) was calculated to be 1.2–1.4 h.[20] Compound **27e** fits the profile that was set as our initial goal: a short-acting DORA. These data suggest that **27e** might be useful as an insomnia drug without the risk of next-day drowsiness. In the near future, we plan to select a clinical candidate with the best profile from among these derivatives.

5. Experimental section

5.1. Biology

5.1.1. Intracellular Ca²⁺ mobilization assay

Chinese hamster ovary (CHO) cells stably expressing the recombinant human OX_1 receptor (hOX_1/CHO) or human OX_2 receptor (hOX_2/CHO) were used in the present study. The cells were seeded into a 96-well black/clear bottom plate (Thermo Fisher Scientific, Rochester, NY) at 2.4×10^4 cells/well and cultured for 18 h. The cells were then incubated with a loading buffer Ca^{2+}-sensitive fluorescent dye, Fluo-4 AM (0.5 μM final concentration; Molecular Probes, Eugene, OR) in an assay buffer containing Hank's balanced salt solution (Life Technologies, Carlsbad, CA), 20 mM HEPES, 0.1% BSA, 2.5 mM probenecid and 0.2 mg/mL amaranth at pH7.4 (loading buffer) at 37 °C for 1 h. The loading buffer was removed, and the cells were washed once with the assay buffer to remove extracellular Fluo-4 AM. Then, the cells were incubated with various concentrations of test compounds for 30 min at room temperature. Intracellular Ca^{2+} mobilization was measured using a Functional Drug Screening System FDSS/μCELL (Hamamatsu Photonics, Shizuoka, Japan).

Responses were measured as the peak increase in fluorescence minus the basal level, normalized to the maximal stimulatory effect induced by the modified human orexin peptide ligand [Ala[6,12]]orexin-A (Peptide Institute, Osaka, Japan). The concentration-response curves were fitted, and the agonist EC_{50} values and the antagonist IC_{50} values were calculated using GraphPad Prism 5.0 (GraphPad Software, San Diego, CA). Then, the K_b values were calculated according to the following equation: $K_b = IC_{50}/(1+[L]/EC_{50})$, where L is the concentration of agonist added to the assay and the IC_{50} and EC_{50} values were derived from the antagonist inhibition and agonist response curves, respectively. The concentration-response curve data shown were the mean with SEM of three individual experiments carried out in duplicate.

5.1.2. Animals

Male Wistar rats (9 weeks old, Charles River Laboratories, Yokohama, Japan) were used to perform the polysomnogram (PSG) study. Male Sprague–Dawley rats (6 weeks old, Charles River Laboratories) were used for the rotarod test. The animals were housed four-to-five per cage under controlled temperature (23 ± 3 °C) and humidity (50 ± 20%) conditions and a 12-h light-dark cycle (lights on 07:00–19:00). Electrode-implanted rats were singly housed before the performance of the PSG study at an age of 11–12 weeks. Food and water were available ad libitum.

All the experimental procedures were reviewed and approved by the Taisho Pharmaceutical Co., Ltd. Animal Care Committee and met the Japanese Experimental Animal Research Association standards, as defined in the Guidelines for Animal Experiments (1987).

5.1.3. Surgical procedures for electrode implantation

Ten-week-old rats were anaesthetized with pentobarbital sodium (50 mg/kg, ip) and fixed on a stereotaxic apparatus. After drilling holes in the skull, stainless steel screw electrodes (E363/20; PlasticsOne, Roanoke, VA) were placed on the cerebral dura mater of the bilateral frontal cortex (as the recording electrode: 2.0 mm anterior, 1.5 mm bilateral from the bregma) and the parietal cortex (as the reference electrode: 6.0 mm posterior, 2.0 mm lateral from the bregma) for the electroencephalogram (EEG) recording, according to a rat brain atlas. To record the electromyogram (EMG), two stainless steel subcutaneous electrodes (E363/76; PlasticsOne) were used, with needles that were bipolarly implanted into the dorsal neck region. These electrodes were socketed into an electrode pedestal (MS363; PlasticsOne) and fixed to the skull with dental resin and superglue. The rats were allowed to recover for 7 days or more before the PSG recording.

5.1.4. Polysomnogram recordings

Rats were weighed and transferred to the measurement cage (width, 220 mm × depth, 300 mm × height, 380 mm; lighting period: 7:00–19:00; free access to food and water) 8–11 h before drug administration. Their electrode pedestal was tethered to a lead wire with a slip ring, and the animals were acclimated to the measurement environment under a freely moving and unrestrained condition. The EEG/EMG recordings were started at 16:00 on the administration day. The test compound and vehicle were administered between 18:50 and 19:00. In addition, the measurements were continued for up to 13 h after administration. The signals from the EEG and EMG electrodes were amplified and passed through bandpass filters (EEG, 0.16–30 Hz; EMG, 5.3–1000 Hz) using a biophysical amplifier (Dia Medical System, Tokyo, Japan). The signals were digitized at a sampling rate of 512 Hz with an analog-to-digital converter (Contec, Osaka, Japan) and were recorded using the data acquisition program SleepSign® ver. 2.0 (Kissei Comtec, Nagano, Japan).

5.1.5. Sleep-wake state determination and data analysis

The sleep-wake states were classified into 8-s epochs as wakefulness, NREM sleep, and REM sleep based on the EEG and EMG patterns, followed by visual verification according to the standard criteria. Each state was characterized as follows: wakefulness, high EMG amplitude and low EEG amplitude; NREM sleep, low EMG amplitude and high EEG amplitude with a high-power density in the delta band (0.5–4.0 Hz); and REM sleep, very low EMG amplitude and low EEG amplitude with high values in the theta band (4.0–8.0 Hz). The cumulative times of wakefulness, NREM sleep, REM sleep, and total sleep (NREM plus REM sleep) during a 2-h period were calculated and were expressed as a percentage of all the states. The latency of sleep was defined as the time from drug administration until the first 15 consecutive 8-s epochs of total sleep.

5.1.6. Rotarod performance

The rotarod (ENV-577; Med Associates, St. Albans, VT), consisted of a gritted plastic roller (3.0 cm in diameter, 8.9 cm long) flanked by two large round plates to prevent the animals from escaping and was run at 10 rpm. All the animals were given control trials prior to the test. A rat was placed on the roller, and the length of time it remained there was measured. A maximum of 2 min was allowed for each animal. The test compound 27e (3–30 mg/kg, ip) and the positive control zolpidem (10 mg/kg, po) were administered 30 min prior to the test.

5.1.7. Statistical analysis

Data from the PSG study (sleep latency and accumulated time of each sleep stage) and rotarod performance (duration time on gritted plastic roller) were expressed as the mean ± SEM. The statistical analysis was performed using SAS System Version 8.2 (SAS Institute Japan, Tokyo, Japan). In the case of the PSG test, the effect of the test compound was analyzed using the Bartlett test (for homogeneity of variance) within the vehicle-treated group and at each dosage of the test compound in the test compound-treated groups. If the variance was homogeneous, then the data were analyzed using the Dunnett test. If the variance was not homogeneous, then the data were analyzed using the Steel test. For the rotarod performance test, the data were statistically evaluated using the Steel test. Values of $P < 0.05$ were regarded as significant.

5.2. Chemistry

5.2.1. General methods

All the solvents and reagents were obtained from commercial suppliers and were used without further purification or were prepared according to published procedures. The ^{1}H and ^{13}C NMR spectra were recorded using a JOEL 500 MHz NMR spectrometer and all the chemical shifts were reported in parts per million (ppm) relative to tetramethylsilane (TMS) as an internal standard. High resolution mass spectral data were acquired using a Shimadzu LCMS-IT-TOF equipped with an ESI/APCI dual ion source. The final compounds exhibited a ⩾95% purity, as determined using HPLC and LC–MS on an Agilent instrument using electrospray ionization. The HPLC conditions were as follows: Shimadzu LC-20A; column Shim-Pack XR-ODS 2.2 µm, 3.0 mm × 75 mm; eluent A, water + 0.1% phosphoric acid; eluent B, acetonitrile; (1) 10% B for 4.0 min, 10–90% B for 5.0 min, 90% B for 2.0 min, (2) 20% B for 4.0 min, 20–90% B for 5.0 min, 90% B for 2.0 min or (3) 40% B for 4.0 min, 40–90% B for 5.0 min, 90% B for 2.0 min; flow rate 0.8 mL/min; UV detection, λ = 210 nm. The LC–MS conditions were as follows: Agilent 1290 infinity and Agilent 6150; column Waters Acquity CSH C18, 1.7 µm, 2.1 mm × 50 mm; eluent A, water + 0.1% formic acid; eluent B, acetonitrile + 0.1% formic acid; 20–99% B for 1.2 min, 99% B for 0.2 min; flow rate 0.8 mL/min; UV detection, λ = 254 nm.

The N-alkylated benzamide orexin receptor antagonists described in this paper exist in two conformations as a result of amide rotamers that are slow on the NMR timescale. The ^{1}H and ^{13}C NMR spectra of compounds 4a–4f, 7, 8, 9, 12, 16, 21, 26a, 26b and 27a–27e consist of broad, overlapping multiplets precluding a detailed coupling constant analysis. Thus, the NMR resonances of these compounds are not listed in numerical format. Instead, pictures of the ^{1}H and ^{13}C NMR spectra of these compounds at 25 °C are included in the Supplementary data. For compound 27e only, the ^{1}H and ^{13}C chemical shifts were assigned based on an analysis of the COSY, HSQC, and HMBC spectra acquired for a sample dissolved in acetone-d_6 at 25 °C.

5.2.2. 5-Fluoro-2-(1H-pyrazol-3-yl)pyridine (2a)

Pd(PPh$_3$)$_4$ (9.23 g, 7.99 mmol) and a 2 mol/L aqueous Na$_2$CO$_3$ solution (2.4 L) were added to an EtOH (1.6 L)/ toluene (1.6 L) mixed solution of 1 (500 g, 1.8 mol) and 2-bromo-5-fluoropyridine (281.2 g, 1.60 mol), and the mixture was heated to 90 °C and stirred for 2 h. After standing to cool at 0 °C, water was added to the reaction mixture, followed by extraction with EtOAc. The extracted organic layer was distilled off under reduced pressure. The obtained residue was stirred in EtOAc (1.2 L), and NH silica gel was added thereto. The mixture was stirred at room temperature for 1 h. Then, the silica gel was filtered off, and the solvent was distilled off under reduced pressure to obtain 5-fluoro-2-(1-(tetrahydro-2H-pyran-2-yl)-1H-pyrazol-5-yl)pyridine as a brown oil.

A 4 mol/L HCl–EtOAc solution (1.2 L) was added to a solution of 5-fluoro-2-(1-(tetrahydro-2H-pyran-2-yl)-1H-pyrazol-5-yl)pyridine in MeOH (1.0 L), and the mixture was stirred at room temperature for 5 h. The deposited solid was then collected by filtration. The obtained solid was stirred in water (2.0 L), and an 8 mol/L aqueous NaOH solution (0.3 L) was added thereto under ice cooling. The mixture was extracted with EtOAc, and the solvent was distilled off under reduced pressure. The obtained residue was stirred for 1 h in Et$_2$O. Then, the deposited solid was collected by filtration and dried by heating under reduced pressure to obtain the title compound 2a as a colorless powder (185 g, 71% over 2 steps). HRMS calcd for C$_8$H$_6$FN$_3$ [M+H]$^+$ 164.0619, found 164.0610. LC–MS t = 0.50 min, [M+H]$^+$ = 164.

^{1}H NMR (500 MHz, CDCl$_3$, 25 °C) δ ppm 6.77 (d, J = 2.06 Hz, 1H), 7.46 (td, J = 8.40, 3.09 Hz, 1H), 7.64 (d, J = 2.06 Hz, 1H), 7.78 (dd, J = 8.75, 4.29 Hz, 1H), 8.48 (d, J = 2.74 Hz, 1H); ^{13}C NMR (500 MHz, CDCl$_3$, 25 °C) δ ppm 103.50, 121.22, 121.26, 123.95, 124.10, 136.71, 137.76, 137.95, 146.38, 158.11, 160.16.

5.2.3. 2-(1H-Pyrazol-3-yl)-5-(trifluoromethyl)pyridine hydrochloride (2b)

The title compound was synthesized according to the procedure described for compound 2a from 2-bromo-5-trifluoromethylpyridine (69% over 2 steps). HRMS calcd for C$_9$H$_6$F$_3$N$_3$ [M+H]$^+$ 214.0587, found 214.0577. LC–MS t = 0.73 min, [M+H]$^+$ = 214.

^{1}H NMR (500 MHz, DMSO-d_6, 25 °C) δ ppm 6.91 (d, J = 2.06 Hz, 1H), 7.81 (d, J = 2.40 Hz, 1H), 8.10–8.13 (m, 1H), 8.20 (dd, J = 8.58, 2.06 Hz, 1H), 8.89–8.93 (m, 1H); ^{13}C NMR (500 MHz, DMSO-d_6, 25 °C) δ ppm 104.77, 119.85, 123.36, 123.80, 124.06, 125.53, 134.92, 146.58, 148.73, 155.70.

5.2.4. 2-(1H-Pyrazol-3-yl)-4-(trifluoromethyl)pyridine hydrochloride (2c)

The title compound was synthesized according to the procedure described for compound 2a from 2-bromo-4-trifluoromethylpyridine (70% over 2 steps). HRMS calcd for C$_9$H$_6$F$_3$N$_3$ [M+H]$^+$ 214.0587, found 214.0581. LC–MS t = 0.71 min, [M+H]$^+$ = 214.

^{1}H NMR (500 MHz, DMSO-d_6, 25 °C) δ ppm 6.94 (d, J = 2.41 Hz, 1H), 7.65 (dt, J = 5.15, 0.86 Hz, 1H), 7.81 (d, J = 2.40 Hz, 1H), 8.17 (s, 1H), 8.83 (d, J = 5.15 Hz, 1H); ^{13}C NMR (500 MHz, DMSO-d_6, 25 °C) δ ppm 104.47, 115.10, 115.13, 118.31, 118.34, 122.40, 124.57, 132.86, 137.70, 137.97, 138.24, 138.51, 148.38, 151.35, 153.30.

5.2.5. 2-(1H-Pyrazol-3-yl)-6-(trifluoromethyl)pyridine (2d)

The title compound was synthesized according to the procedure described for compound 2a from 2-bromo-6-trifluoromethylpyridine (48% over 2 steps). HRMS calcd for C$_9$H$_6$F$_3$N$_3$ [M+H]$^+$ 214.0587, found 214.0575. LC–MS t = 0.90 min, [M+H]$^+$ = 214.

^{1}H NMR (500 MHz, CDCl$_3$, 25 °C) δ ppm 6.92 (d, J = 1.71 Hz, 1H), 7.59 (d, J = 8.58 Hz, 1H), 7.68 (d, J = 2.06 Hz, 1H), 7.87–7.93 (m, 1H), 7.94–7.99 (m, 1H); ^{13}C NMR (500 MHz, CDCl$_3$, 25 °C) δ ppm 104.44, 118.20, 119.21, 120.38, 122.55, 124.75, 136.31, 138.29, 147.67, 147.95, 148.23, 148.51, 150.39.

5.2.6. 2-Methyl-6-(1H-pyrazol-3-yl)pyridine (2e)

The title compound was synthesized according to the procedure described for compound 2a from 2-bromo-6-trifluoromethylpyridine (35% over 2 steps). HRMS calcd for C$_9$H$_9$N$_3$ [M+H]$^+$ 160.0869, found 160.0878. LC–MS t = 0.24 min, [M+H]$^+$ = 160.

^{1}H NMR (500 MHz, CDCl$_3$, 25 °C) δ ppm 2.57 (s, 3H), 6.74 (d, J = 1.72 Hz, 1H), 7.07 (d, J = 7.89 Hz, 1H), 7.49 (d, J = 7.89 Hz, 1H), 7.57–7.62 (m, 1H), 7.63 (d, J = 2.06 Hz, 1H); ^{13}C NMR (500 MHz, CDCl$_3$, 25 °C) δ ppm 24.51, 103.16, 105.12, 117.16, 122.49, 137.16, 138.31, 148.39, 158.44.

5.2.7. N-Ethyl-2-[3-(5-fluoropyridin-2-yl)-1H-pyrazol-1-yl]ethanamine dihydrochloride (3a)

A solution of 3-ethyl-1,2,3-oxathiazolidine-2,2-dioxide (2.22 g, 14.7 mmol) in CH$_3$CN (5.0 mL) was added dropwise to a mixture of 5-fluoro-2-(1H-pyrazol-3-yl)pyridine (2.00 g, 12.3 mmol), NaOH (0.74 g, 18.4 mmol), and CH$_3$CN (15 mL) at 70 °C, and the mixture was stirred at the same temperature as above for 1 h. After ice cooling, 25% H$_2$SO$_4$ (12 mL) was added thereto at 25 °C. The reaction mixture was heated and stirred at 70 °C for 4 h. After ice cooling, an 8 mol/L aqueous NaOH solution was added thereto, and the mixture was then separated into aqueous and organic layers. The solvent in the organic layer was distilled off under reduced pressure. The residue was stirred in EtOAc (20 mL), and a 4 mol/L HCl–EtOAc solution (4.6 mL) was added thereto under ice cooling. The mixture was stirred at room temperature for 1 h, and the

deposited solid was then collected by filtration. The obtained solid was dried by heating under reduced pressure to obtain the title compound **3a** as a colorless powder (2.7 g, 72%). HRMS calcd for $C_{12}H_{15}FN_4$ [M+H]$^+$ 235.1354, found 235.1347. LC–MS t = 0.26 min, [M+H]$^+$ = 235.

^{1}H NMR (500 MHz, DMSO-d_6, 25 °C) δ ppm 1.17 (t, J = 7.38 Hz, 3H), 2.87–2.97 (m, 2H), 3.38 (quin, J = 6.26 Hz, 2H), 4.53 (t, J = 6.52 Hz, 2H), 6.81 (d, J = 2.06 Hz, 1H), 7.77 (td, J = 8.75, 2.74 Hz, 1H), 7.90 (d, J = 2.40 Hz, 1H), 7.98 (dd, J = 8.75, 4.63 Hz, 1H), 8.55 (d, J = 3.09 Hz, 1H); ^{13}C NMR (500 MHz, DMSO-d_6, 25 °C) δ ppm 11.37, 42.65, 46.08, 48.02, 104.82, 121.47, 121.50, 124.74, 124.90, 133.41, 137.35, 137.54, 148.70, 150.97, 158.00, 160.02.

5.2.8. *N*-Ethyl-2-{3-[5-(trifluoromethyl)pyridin-2-yl]-1*H*-pyrazol-1-yl}ethanamine dihydrochloride (3b)

The title compound was synthesized according to the procedure described for compound **3a** from 2-(1*H*-pyrazol-3-yl)-5-(trifluoromethyl)pyridine hydrochloride **2b** (45%). HRMS calcd for $C_{13}H_{15}F_3N_4$ [M+H]$^+$ 285.1322, found 285.1307. LC–MS t = 0.41 min, [M+H]$^+$ = 285.

^{1}H NMR (500 MHz, DMSO-d_6, 25 °C) δ ppm 1.01–1.29 (m, 3H), 2.80–3.08 (m, 2H), 3.42 (quin, J = 6.17 Hz, 2H), 4.54 (t, J = 6.35 Hz, 2H), 6.94 (d, J = 2.40 Hz, 1H), 7.95 (d, J = 2.40 Hz, 1H), 8.11 (d, J = 8.23 Hz, 1H), 8.22 (dd, J = 8.40, 2.23 Hz, 1H), 8.93 (dd, J = 1.37, 0.69 Hz, 2H); ^{13}C NMR (500 MHz, DMSO-d_6, 25 °C) δ ppm 11.40, 42.74, 46.11, 48.30, 105.82, 119.93, 123.33, 124.02, 124.28, 125.51, 133.75, 134.88, 134.90, 146.71, 146.74, 150.80, 155.70.

5.2.9. *N*-Ethyl-2-{3-[4-(trifluoromethyl)pyridin-2-yl]-1*H*-pyrazol-1-yl}ethanamine dihydrochloride (3c)

The title compound was synthesized according to the procedure described for compound **3a** from 2-(1*H*-pyrazol-3-yl)-4-(trifluoromethyl)pyridine hydrochloride **2c** (85%). HRMS calcd for $C_{13}H_{15}F_3N_4$ [M+H]$^+$ 285.1322, found 285.1311. LC–MS t = 0.28 min, [M+H]$^+$ = 285.

^{1}H NMR (500 MHz, DMSO-d_6, 25 °C) δ ppm 1.17 (t, J = 7.20 Hz, 3H), 2.85–3.00 (m, 2H), 3.41 (quin, J = 6.17 Hz, 2H), 4.55 (t, J = 6.35 Hz, 2H), 6.93 (d, J = 2.06 Hz, 1H), 7.67 (d, J = 4.12 Hz, 1H), 7.96 (d, J = 2.40 Hz, 1H), 8.14 (s, 1H), 8.84 (d, J = 5.15 Hz, 1H); ^{13}C NMR (500 MHz, DMSO-d_6, 25 °C) δ ppm 11.37, 42.68, 46.07, 48.20, 105.36, 114.98, 115.01, 118.48, 118.51, 120.25, 122.43, 124.60, 126.78, 133.80, 137.50, 137.77, 138.04, 138.31, 150.75, 151.62, 153.52.

5.2.10. *N*-Ethyl-2-{3-[6-(trifluoromethyl)pyridin-2-yl]-1*H*-pyrazol-1-yl}ethanamine hydrochloride (3d)

The title compound was synthesized according to the procedure described for compound **3a** from 2-(1*H*-pyrazol-3-yl)-6-(trifluoromethyl)pyridine **2d** (44%). HRMS calcd for $C_{13}H_{15}F_3N_4$ [M+H]$^+$ 285.1322, found 285.1314. LC–MS t = 0.45 min, [M+H]$^+$ = 285.

^{1}H NMR (500 MHz, DMSO-d_6, 25 °C) δ ppm 0.97–1.34 (m, 3H), 2.93 (q, J = 7.32 Hz, 2H), 3.40 (t, J = 6.35 Hz, 2H), 4.54 (t, J = 6.35 Hz, 2H), 6.88 (d, J = 2.40 Hz, 1H), 7.79 (dd, J = 7.55, 0.69 Hz, 1H), 7.94 (d, J = 2.40 Hz, 1H), 8.07–8.14 (m, 1H), 8.15–8.22 (m, 1H); ^{13}C NMR (500 MHz, DMSO-d_6, 25 °C) δ ppm 11.41, 42.71, 46.14, 48.23, 105.40, 119.90, 121.04, 123.22, 123.51, 125.41, 133.66, 139.75, 146.42, 146.69, 146.96, 147.22, 150.63, 152.80.

5.2.11. *N*-Ethyl-2-[3-(6-methylpyridin-2-yl)-1*H*-pyrazol-1-yl]ethanamine dihydrochloride (3e)

The title compound was synthesized according to the procedure described for compound **3a** from 2-methyl-6-(1*H*-pyrazol-3-yl)pyridine **2e** (44%). HRMS calcd for $C_{13}H_{18}N_4$ [M+H]$^+$ 231.1604, found 231.1593. LC–MS t = 0.25 min, [M+H]$^+$ = 231.

^{1}H NMR (500 MHz, DMSO-d_6, 25 °C) δ ppm 1.21 (t, J = 7.20 Hz, 3H), 2.75 (s, 3H), 2.87–3.04 (m, 2H), 3.41 (quin, J = 6.17 Hz, 2H), 4.62 (t, J = 6.17 Hz, 2H), 7.27 (br s, 1H), 7.54–7.68 (m, 1H), 8.04 (d, J = 2.40 Hz, 1H), 8.11 (d, J = 7.20 Hz, 1H), 8.25 (d, J = 0.69 Hz, 1H); ^{13}C NMR (500 MHz, DMSO-d_6, 25 °C) δ ppm 11.33, 21.32, 42.81, 45.94, 48.35, 106.99, 120.58, 125.65, 134.20, 144.11, 146.84, 155.90.

5.2.12. *N*-Ethyl-2-[3-(4-fluorophenyl)-1*H*-pyrazol-1-yl]ethanamine dihydrochloride (3f)

The title compound was synthesized according to the procedure described for compound **3a** from 3-(4-fluorophenyl)-1*H*-pyrazole **2f** (59%). HRMS calcd for $C_{13}H_{16}FN_3$ [M+H]$^+$ 234.1401, found 234.1383. LC–MS t = 0.39 min, [M+H]$^+$ = 234.

^{1}H NMR (500 MHz, DMSO-d_6, 25 °C) δ ppm 1.16 (t, J = 7.20 Hz, 3H), 2.87–2.97 (m, 2H), 3.36 (quin, J = 6.26 Hz, 2H), 4.48 (t, J = 6.35 Hz, 2H), 6.73 (d, J = 2.40 Hz, 1H), 7.20 (t, J = 8.92 Hz, 2H), 7.79–7.87 (m, 3H); ^{13}C NMR (500 MHz, DMSO-d_6, 25 °C) δ ppm 11.40, 42.65, 46.13, 47.84, 103.47, 115.93, 116.10, 127.65,127.71, 130.26, 130.29, 133.22, 150.48, 161.29, 163.23.

5.2.13. *N*-Ethyl-*N*-{2-[3-(5-fluoropyridin-2-yl)-1*H*-pyrazol-1-yl]ethyl}-2-(2*H*-1,2,3-triazol-2-yl)benzamide (27e)

1-(3-Dimethylaminopropyl)-3-ethylcarbodiimide hydrochloride (WSC·HCl) (37.4 g, 0.20 mol) was added to a solution of *N*-ethyl-2[3-(5-fluoro-pyridin-2-yl)-1*H*-pyrazol-1-yl] ethanamine dihydrochloride (50 g, 0.16 mol), 5-methyl-2-(2*H*-1,2,3-triazol-2-yl)benzoic acid (33.9 g, 0.18 mol), 1-hydroxy-1*H*-benzotriazole hydrate (HOBt·H$_2$O) (26.4 g, 0.20 mol) and triethylamine (TEA) (39.5 g, 0.39 mol) in THF (500 mL) at 0 °C, followed by stirring at room temperature for 20.5 h. The solvent of the reaction solution was distilled off under reduced pressure. An aqueous NaHCO$_3$ solution and EtOAc were added to the resulting residue, followed by extraction with EtOAc. The organic layer was washed with water, and the solvent was distilled off under reduced pressure to yield the crude product (72 g). An additional 196.7 g of the crude product was synthesized using the same method from *N*-ethyl-2[3-(5-fluoro-pyridin-2-yl)-1*H*-pyrazol-1-yl] ethanamine dihydrochloride (140 g, 0.46 mol) and 5-methyl-2-(2*H*-1,2,3-triazol-2-yl)benzoic acid (94.8 g, 0.50 mol). The obtained crude product (268.7 g) was recrystallized with heptane and EtOAc. The deposited solid was then collected by filtration. The obtained solid was dried by heating under reduced pressure to yield the title compound **27e** as a colorless powder (217.3 g). HRMS calcd for $C_{21}H_{20}FN_7O$ [M+H]$^+$ 406.1786, found 406.1805. LC–MS t = 0.95 min, [M+H]$^+$ = 406.

Compound **27e** exists as a mixture of two rotameric components in chemical exchange in acetone-d_6 at room temperature (1:0.57). The ^{1}H and ^{13}C chemical shifts of the two rotamers were assigned based on an analysis of the COSY, HSQC, and HMBC spectra acquired for a sample dissolved in acetone-d_6 at 25 °C.

Rotamer 1 (64% of total): ^{1}H NMR (500 MHz, acetone-d_6, 25 °C) δ ppm 0.90 (3H), 3.02–3.14 (2H), 3.87–3.97 (2H), 4.39–4.51 (1H), 4.57–4.67 (1H), 6.87 (1H), 7.47–7.53 (2H), 7.58–7.67 (2H), 7.84 (1H), 8.00 (1H), 8.01 (2H), 8.11 (1H), 8.48 (1H).

^{13}C NMR (500 MHz, acetone-d_6, 25 °C) δ ppm 13.33, 44.92, 45.76, 49.95, 104.77, 104.80, 121.35, 123.03, 124.22, 128.82, 128.94, 130.49, 131.05, 131.09, 132.82, 132.87, 136.95, 137.13, 137.80, 150.16, 151.92, 160.72, 169.54.

Rotamer 2 (36% of total): ^{1}H NMR (500 MHz, acetone-d_6, 25 °C) δ ppm 1.19 (3H), 3.16–3.25 (1H), 3.49–3.57 (1H), 3.65–3.75 (1H), 3.79–3.87 (1H), 4.22–4.28 (1H), 4.39–4.51 (1H), 6.83 (1H), 6.91 (1H), 7.17 (1H), 7.47–7.53 (1H), 7.58–7.67 (1H), 7.64 (1H), 7.89 (1H), 7.92 (1H), 7.96 (2H), 8.48 (1H).

^{13}C NMR (500 MHz, acetone-d_6, 25 °C) δ ppm 11.45, 39.56, 48.72, 50.70, 104.77, 104.80, 121.46, 122.80, 124.08, 128.82,

129.06, 130.14, 131.05, 131.09, 132.82, 132.87, 136.83, 136.90, 137.61, 150.00, 152.10, 158.71, 169.24.

5.2.14. *N*-Ethyl-*N*-{2-[3-(5-fluoropyridin-2-yl)-1*H*-pyrazol-1-yl]ethyl}-5-methyl-2-(2*H*-1,2,3-triazol-2-yl)benzamide (4a)

TEA (1.20 mL, 8.63 mmol) was added to a solution of *N*-ethyl-2[3-(5-fluoro-pyridin-2-yl)-1*H*-pyrazol-l-yl] ethanamine dihydrochloride (0.50 g, 1.63 mmol) in CHC1₃ (5 mL) at room temperature. 5-methyl-2-(2*H*-1,2,3-triazol-2-yl)benzoic acid (0.36 g, 1.79 mmol) and propylphosphonic acid anhydride (cyclic trimer) (50% solution in DMF [approximately 1.6 mol/L], 1.32 mL, 2.12 mmol) were added to the reaction solution under cooling in ice water. The resultant mixture was stirred at 50 °C for 5 h. After standing until cooled to room temperature, water was added thereto, followed by extraction with CHCl₃. The organic layer was washed with brine. Then, the organic layer was dried over MgSO₄ and the desiccant was filtered off. Then, the solvent was distilled off under reduced pressure. The obtained residue was purified by column chromatography (20–80% EtOAc in hexanes) and washed with Et₂O to yield the title compound **4a** as a colorless powder (0.51 g, 75%). HRMS calcd for $C_{22}H_{22}FN_7O$ [M+H]$^+$ 420.1943, found 420.1936. LC–MS t = 1.00 min, [M+H]$^+$ = 420. Please see the Supplementary data for pictures of 500 MHz ^{1}H and 500 MHz ^{13}C NMR spectra in acetone-d_6 at 25 °C.

5.2.15. *N*-Ethyl-5-methyl-2-(2*H*-1,2,3-triazol-2-yl)-*N*-(2-{3-[5-(trifluoromethyl)pyridin-2-yl]-1*H*-pyrazol-1-yl}ethyl)benzamide (4b)

The title compound was synthesized according to the procedure described for compound **27e** from *N*-ethyl-2-{3-[5-(trifluoromethyl)pyridin-2-yl]-1*H*-pyrazol-1-yl}ethanamine dihydrochloride **3b** and 5-methyl-2-(2*H*-1,2,3-triazol-2-yl)benzoic acid (52%). HRMS calcd for $C_{23}H_{22}F_3N_7O$ [M+H]$^+$ 470.1911, found 470.1901. LC–MS t = 1.07 min, [M+H]$^+$ = 470. Please see the Supplementary data for pictures of 500 MHz ^{1}H and 500 MHz ^{13}C NMR spectra in acetone-d_6 at 25 °C.

5.2.16. *N*-Ethyl-5-methyl-2-(2*H*-1,2,3-triazol-2-yl)-*N*-(2-{3-[4-(trifluoromethyl)pyridin-2-yl]-1*H*-pyrazol-1-yl}ethyl)benzamide (4c)

The title compound was synthesized according to the procedure described for compound **27e** from *N*-ethyl-2-{3-[4-(trifluoromethyl)pyridin-2-yl]-1*H*-pyrazol-1-yl}ethanamine dihydrochloride **3c**, 5-methyl-2-(2*H*-1,2,3-triazol-2-yl)benzoic acid and HATU which was used as condensation agent instead of WSC·HCl (62%). HRMS calcd for $C_{23}H_{22}F_3N_7O$ [M+H]$^+$ 470.1911, found 470.1900. LC–MS t = 1.06 min, [M+H]$^+$ = 470. Please see the Supplementary data for pictures of 500 MHz ^{1}H and 500 MHz ^{13}C NMR spectra in acetone-d_6 at 25 °C.

5.2.17. *N*-Ethyl-5-methyl-2-(2*H*-1,2,3-triazol-2-yl)-*N*-(2-{3-[6-(trifluoromethyl)pyridin-2-yl]-1*H*-pyrazol-1-yl}ethyl)benzamide (4d)

The title compound was synthesized according to the procedure described for compound **4a** from *N*-ethyl-2-{3-[6-(trifluoromethyl)pyridin-2-yl]-1*H*-pyrazol-1-yl}ethanamine hydrochloride **3d** and 5-methyl-2-(2*H*-1,2,3-triazol-2-yl)benzoic acid (78%). HRMS calcd for $C_{23}H_{22}F_3N_7O$ [M+H]$^+$ 470.1911, found 470.1896. LC–MS t = 1.19 min, [M+H]$^+$ = 470. Please see the Supplementary data for pictures of 500 MHz ^{1}H and 500 MHz ^{13}C NMR spectra in acetone-d_6 at 25 °C.

5.2.18. *N*-Ethyl-5-methyl-*N*-{2-[3-(6-methylpyridin-2-yl)-1*H*-pyrazol-1-yl]ethyl}-2-(2*H*-1,2,3-triazol-2-yl)benzamide (4e)

The title compound was synthesized according to the procedure described for compound **4a** from *N*-ethyl-2-[3-(6-methylpyridin-2-yl)-1*H*-pyrazol-1-yl]ethanamine dihydrochloride **3e** and 5-methyl-2-(2*H*-1,2,3-triazol-2-yl)benzoic acid (47%). HRMS calcd for $C_{23}H_{25}N_7O$ [M+H]$^+$ 416.2193, found 416.2185. LC–MS t = 0.52–0.64 min, [M+H]$^+$ = 416. Please see the Supplementary data for pictures of 500 MHz ^{1}H and 500 MHz ^{13}C NMR spectra in acetone-d_6 at 25 °C.

5.2.19. *N*-Ethyl-*N*-{2-[3-(4-fluorophenyl)-1*H*-pyrazol-1-yl]ethyl}-5-methyl-2-(2*H*-1,2,3-triazol-2-yl)benzamide (4f)

The title compound was synthesized according to the procedure described for compound **4a** from *N*-ethyl-2-[3-(4-fluorophenyl)-1*H*-pyrazol-1-yl]ethanamine dihydrochloride **3f** and 5-methyl-2-(2*H*-1,2,3-triazol-2-yl)benzoic acid (88%). HRMS calcd for $C_{23}H_{23}FN_6O$ [M+H]$^+$ 419.1990, found 419.1980. LC–MS t = 1.16 min, [M+H]$^+$ = 419. Please see the Supplementary data for pictures of 500 MHz ^{1}H and 500 MHz ^{13}C NMR spectra in acetone-d_6 at 25 °C.

5.2.20. *N*-Ethyl-5-fluoro-*N*-{2-[3-(5-fluoropyridin-2-yl)-1*H*-pyrazol-1-yl]ethyl}-2-(2*H*-1,2,3-triazol-2-yl)benzamide (27a)

The title compound was synthesized according to the procedure described for compound **27e** from 5-fluoro-2-(2*H*-1,2,3-triazol-2-yl)benzoic acid (60%). HRMS calcd for $C_{21}H_{19}F_2N_7O$ [M+H]$^+$ 424.1692, found 424.1687. LC–MS t = 0.93 min, [M+H]$^+$ = 424. Please see the Supplementary data for pictures of 500 MHz ^{1}H and 500 MHz ^{13}C NMR spectra in acetone-d_6 at 25 °C.

5.2.21. 5-Chloro-*N*-ethyl-*N*-{2-[3-(5-fluoropyridin-2-yl)-1*H*-pyrazol-1-yl]ethyl}-2-(2*H*-1,2,3-triazol-2-yl)benzamide (27b)

The title compound was synthesized according to the procedure described for compound **4a** from 5-chloro-2-(2*H*-1,2,3-triazol-2-yl)benzoic acid (42%). HRMS calcd for $C_{21}H_{19}ClFN_7O$ [M+H]$^+$ 440.1396, found 440.1390. LC–MS t = 0.93–1.05 min, [M+H]$^+$ = 440. Please see the Supplementary data for pictures of 500 MHz ^{1}H and 500 MHz ^{13}C NMR spectra in acetone-d_6 at 25 °C.

5.2.22. *N*-Ethyl-*N*-{2-[3-(5-fluoropyridin-2-yl)-1*H*-pyrazol-1-yl]ethyl}-5-methoxy-2-(2*H*-1,2,3-triazol-2-yl)benzamide (27c)

The title compound was synthesized according to the procedure described for compound **4a** from 5-methoxy-2-(2*H*-1,2,3-triazol-2-yl)benzoic acid (44%). HRMS calcd for $C_{22}H_{22}FN_7O_2$ [M+H]$^+$ 436.1892, found 436.1878. LC–MS t = 0.98 min, [M+H]$^+$ = 436. Please see the Supplementary data for pictures of 500 MHz ^{1}H and 500 MHz ^{13}C NMR spectra in acetone-d_6 at 25 °C.

5.2.23. *N*-Ethyl-*N*-{2-[3-(5-fluoropyridin-2-yl)-1*H*-pyrazol-1-yl]ethyl}-5-methyl-2-(pyrimidin-2-yl)benzamide (27d)

The title compound was synthesized according to the procedure described for compound **4a** from 5-methyl-2-(pyrimidin-2-yl)benzoic acid (36%). HRMS calcd for $C_{24}H_{23}FN_6O$ [M+H]$^+$ 431.1990, found 431.2001. LC–MS t = 0.98 min, [M+H]$^+$ = 431. Please see the Supplementary data for pictures of 500 MHz ^{1}H and 500 MHz ^{13}C NMR spectra in acetone-d_6 at 25 °C.

5.2.24. *N*-Ethyl-*N*-(2-hydroxyethyl)-5-methyl-2-(2*H*-1,2,3-triazol-2-yl)benzamide (7)

To a suspension of 5-methyl-2-(2*H*-1,2,3-triazol-2-yl)benzoic acid (2.0 g, 9.84 mmol) in CHCl₃ (20 mL) was added SOCl₂ (1.1 mL, 14.8 mmol) at 0 °C. The reaction mixture was heated to reflux for 1 h. After standing until cooled to room temperature, the solvent in the reaction mixture was distilled off under reduced pressure. TEA (2.7 mL, 19.7 mmol) and 2-(ethylamino)ethanol (1.2 mL, 10.8 mmol) were then added to a solution of the residue obtained in the previous step in CHCl₃ (20 mL) at 0 °C. The solution was stirred for 16 h at room temperature. An aqueous NaHCO₃ solution and water were added to the reaction mixture, followed

by extraction with CHCl$_3$. The organic layer was washed with brine and was dried over MgSO$_4$. The desiccant was then removed by filtration, and the solvent was distilled off under reduced pressure. The obtained residue was purified by column chromatography (20–80% EtOAc in hexanes) to yield the title compound **7** as a colorless oil (2.4 g, 89%). HRMS calcd for C$_{14}$H$_{18}$N$_4$O$_2$ [M+H]$^+$ 275.1503, found 275.1503. LC–MS t = 0.62–0.73 min, [M+H]$^+$ = 275. Please see the Supplementary data for pictures of 500 MHz ^{1}H and 500 MHz ^{13}C NMR spectra in CDCl$_3$ at 25 °C.

5.2.25. N-(2-Cyanoethyl)-N-ethyl-5-methyl-2-(2H-1,2,3-triazol-2-yl)benzamide (8)

Methanesulfonyl chloride (MsCl) (0.30 mL, 3.83 mmol) was added to a solution of compound **7** (1.0 g, 3.65 mmol) and TEA (0.76 mL, 5.47 mmol) in CHCl$_3$ (10 mL) under cooling in ice water, and the mixture was heated to room temperature and stirred for 1 h. Water was then added under cooling in ice water, followed by extraction with CHCl$_3$. Next, the organic layer was washed with brine and allowed to pass through an ISOLUTE® Phase Separator. Then, the filtrate was concentrated under reduced pressure. NaCN (0.27 g, 5.47 mmol) was added to a solution of the obtained residue in DMF (10 mL), and the mixture was stirred in an oil bath with a temperature of 80 °C for 3.5 h. After standing until cooled to room temperature, water was added thereto, followed by extraction with EtOAc. The organic layer was washed with brine and was dried with MgSO$_4$. The desiccant was then removed by filtration, and the solvent was distilled off under reduced pressure. The obtained residue was purified by column chromatography (20–80% EtOAc in hexanes) to yield the title compound **8** as a colorless powder (0.96 g, 93% over 2 steps). HRMS calcd for C$_{15}$H$_{17}$N$_5$O [M+H]$^+$ 284.1506, found 284.1512. LC–MS t = 0.86 min, [M+H]$^+$ = 284. Please see the Supplementary data for pictures of 500 MHz ^{1}H and 500 MHz ^{13}C NMR spectra in CDCl$_3$ at 25 °C.

5.2.26. N-Ethyl-N-{2-[5-(5-fluoropyridin-2-yl)-1,2,4-oxadiazol-3-yl]ethyl}-5-methyl-2-(2H-1,2,3-triazol-2-yl)benzamide (9)

An aqueous 50% hydroxylamine solution (0.31 mL, 5.29 mmol) was added to a solution of N-(2-cyanoethyl)-N-ethyl-5-methyl-2-(2H-1,2,3-triazol-2-yl)benzamide **8** (0.50 g, 1.76 mmol) in EtOH (10 mL), followed by stirring at 80 °C for 4 h. After cooling at room temperature, the reaction solution was concentrated under reduced pressure. Water was added to the obtained residue, followed by extraction with EtOAc. The organic layer was washed with brine and was dried over MgSO$_4$. The desiccant was then removed by filtration, and the solvent was distilled off under reduced pressure. A solution of the resulting residue in CH$_3$CN (5 mL) and DMF (0.5 mL) was added to a solution of 5-fluoropyridin-2-carboxylic acid (0.27 g, 1.95 mmol) and carbonyldiimidazole (0.34 g, 2.12 mmol) in CH$_3$CN (5 mL) and DMF (0.5 mL) that was then stirred in advance at room temperature for 3 h. The reaction solution was stirred for 2 h at room temperature. Next, 1,8-diazabicyclo[5.4.0]undec-7-ene (DBU) (0.26 mL, 1.77 mmol) was added to the reaction mixture, followed by stirring at 70 °C for 1 h. After cooling at room temperature, water was added to the reaction mixture, followed by extraction with EtOAc. The organic layer was washed with a 1.2 mol/L aqueous HCl solution and brine and was dried over MgSO$_4$. The desiccant was then removed by filtration, and the solvent was distilled off under reduced pressure. The resulting residue was purified by column chromatography (20–80% EtOAc in hexanes) and washed with Et$_2$O to give the title compound **9** as a colorless powder (0.47 g, 63% over 2 steps). HRMS calcd for C$_{21}$H$_{20}$FN$_7$O$_2$ [M+H]$^+$ 422.1735, found 422.1739. LC–MS t = 0.98 min, [M+H]$^+$ = 422. Please see the Supplementary data for pictures of 500 MHz ^{1}H and ^{13}C NMR spectra in acetone-d_6 at 25 °C.

5.2.27. 5-Fluoro-2-(1H-pyrazol-4-yl)pyridine (11)

A 2 mol/L aqueous Na$_2$CO$_3$ solution (45.2 g, 426.2 mmol) and Pd(PPh$_3$)$_4$ (4.93 g, 4.26 mmol) were added to a solution of tert-butyl 4-(4,4,5,5-tetramethyl-1,3,2-dioxaborolan-2-yl)-1H-pyrazole-1-carboxylate (46.0 g, 156.3 mmol) and 2-bromo-5-fluoropyridine (25.0 g, 142.1 mmol) in 1,4-dioxane (284 mL). The mixture was then stirred in an oil bath with a temperature of 90 °C for 4 h. Next, the mixture was stirred at room temperature for 2 days. Brine was added to the reaction mixture, followed by extraction with EtOAc. The organic layer was dried over Na$_2$SO$_4$, and the desiccant was filtered off. Then, the solvent was distilled off under reduced pressure. EtOAc was added to the obtained residue, and the deposited solid was collected by filtration to obtain the title compound **11** as a colorless powder (13.0 g, 56%). HRMS calcd for C$_8$H$_6$FN$_3$ [M+H]$^+$ 164.0619, found 164.0620. LC–MS t = 0.52 min, [M+H]$^+$ = 164.

^{1}H NMR (500 MHz, CDCl$_3$, 25 °C) δ ppm 7.36–7.44 (m, 1H), 7.49 (dd, J = 8.75, 4.29 Hz, 1H), 8.06 (s, 2H), 8.43 (d, J = 2.74 Hz, 1H); ^{13}C NMR (500 MHz, CDCl$_3$, 25 °C) δ ppm 120.51, 120.55, 122.59, 123.57, 123.72, 132.37, 137.69, 137.88, 148.25, 148.28, 157.10, 159.13.

5.2.28. N-Ethyl-N-{2-[4-(5-fluoropyridin-2-yl)-1H-pyrazol-1-yl]ethyl}-5-methyl-2-(2H-1,2,3-triazol-2-yl)benzamide (12)

MsCl (0.15 mL, 1.91 mmol) was added to a solution of compound **7** (0.50 g, 1.82 mmol) and TEA (0.38 mL, 2.73 mmol) in CHCl$_3$ (2 mL) under cooling in ice water, and the mixture was warmed to room temperature and stirred for 1 h. Water was then added under cooling in ice water, followed by extraction with CHCl$_3$. Next, the organic layer was washed with brine and allowed to pass through an ISOLUTE® Phase Separator. Then, the filtrate was concentrated under reduced pressure. Cs$_2$CO$_3$ (1.31 g, 4.01 mmol) was added to a solution of the obtained residue and compound **11** (0.33 g, 2.00 mmol) in DMF (2 mL), and the mixture was stirred in an oil bath with a temperature of 80 °C for 4 h. After standing until cooled to room temperature, water was added thereto, followed by extraction with EtOAc. The organic layer was washed with brine and was dried over MgSO$_4$. The desiccant was then removed by filtration, and the solvent was distilled off under reduced pressure. The obtained residue was purified by column chromatography (20–80% EtOAc in hexanes) and washed with Et$_2$O to yield the title compound **12** as a colorless powder (0.30 g, 39% over 2 steps). HRMS calcd for C$_{22}$H$_{22}$FN$_7$O [M+H]$^+$ 420.1943, found 420.1939. LC–MS t = 0.98 min, [M+H]$^+$ = 420.

Please see the Supplementary data for pictures of 500 MHz ^{1}H and ^{13}C NMR spectra in acetone-d_6 at 25 °C.

5.2.29. N-{2-[5-(5-Fluoropyridin-2-yl)-1,2-oxazol-3-yl]ethyl}-5-methyl-2-(2H-1,2,3-triazol-2-yl)benzamide (15)

HATU (1.94 g, 5.09 mmol) was added to a solution of 3,3-diethoxypropan-1-amine (0.50 g, 3.40 mmol), 5-methyl-2-(2H-1,2,3-triazol-2-yl)benzoic acid (0.83 g, 4.08 mmol) and N,N-diisopropylethylamine (DIPEA) (2.97 mL, 17.0 mmol) in DMF (5 mL), followed by stirring at room temperature for 15 h. An aqueous NaHCO$_3$ solution was added to the reaction solution, followed by extraction with EtOAc. The organic layer was washed with brine and was dried with MgSO$_4$. The desiccant was then removed by filtration, and the solvent was distilled off under reduced pressure. The resulting residue was purified by column chromatography (20–80% EtOAc in hexanes) to yield N-(3,3-diethoxy-propyl)-5-methyl-2-(2H-1,2,3-triazol-2-yl)benzamide **14** as a brown oil (1.13 g, 100%).

An aqueous 1.2 mol/L HCl solution was then added to a solution of compound **14** (0.82 g, 2.47 mmol) in THF (10 mL), followed by stirring at room temperature for 18 h. An aqueous NaHCO$_3$ solution was added to the reaction solution to adjust the pH to a neutral level, followed by extraction with EtOAc. The organic layer

was washed with brine and was dried over MgSO$_4$. The desiccant was then removed by filtration, and the solvent was distilled off under reduced pressure. Sodium acetate (0.28 g, 3.45 mmol) and hydroxylamine hydrochloride (0.24 g, 3.45 mmol) were added to an aqueous solution of the residue in 95% EtOH (10 mL), followed by stirring in an ice bath for 3 h. An aqueous NaHCO$_3$ solution was added to the reaction solution, followed by extraction with EtOAc. The organic layer was washed with brine and was dried over MgSO$_4$. The desiccant was then removed by filtration, and the solvent was distilled off under reduced pressure. The resulting solid was washed with Et$_2$O and was then collected by filtration to give N-[3-(hydroxyimino)propyl]-5-methyl-2-(2H-1,2,3-triazol-2-yl)benzamide as a colorless powder (0.23 g).

N-Chlorosuccinimide (0.081 g, 0.60 mmol) was added to a solution of N-[3-(hydroxylimino)propyl]-5-methyl-2-(2H-1,2,3-triazol-2-yl)benzamide (0.15 g, 0.55 mmol) in DMF (2 mL) in an ice bath. The mixture was warmed to room temperature, followed by stirring for 16 h. Water was added to the reaction solution, followed by extraction with EtOAc. The organic layer was washed with brine and was dried over MgSO$_4$. The desiccant was then removed by filtration, and the solvent was distilled off under reduced pressure. The residue was dissolved in THF (4 mL), and a solution of 2-ethynyl-5-fluoropyridine (0.10 g, 0.83 mmol) in THF (1 mL) was dropwise added to the solution in an ice bath. TEA (0.084 mL, 0.83 mmol) was further dropwise added thereto. The mixture was warmed to room temperature, followed by stirring for 16 h. Water was added to the reaction solution, followed by extraction with EtOAc. The organic layer was washed with brine and was dried over MgSO$_4$. The desiccant was then removed by filtration, and the solvent was distilled off under reduced pressure. The resulting residue was purified by column chromatography (20–80% EtOAc in hexanes) to give the title compound 15 as a colorless powder (0.050 g, 8% over 4 steps). HRMS calcd for C$_{20}$H$_{17}$FN$_6$O$_2$ [M+H]$^+$ 393.1470, found 393.1466. LC–MS t = 0.85 min, [M+H]$^+$ = 393.

^{1}H NMR (500 MHz, CDCl$_3$, 25 °C) δ ppm 2.37–2.44 (m, 3H), 2.96 (t, J = 6.52 Hz, 2H), 3.74 (q, J = 6.17 Hz, 2H), 6.24 (t, J = 5.32 Hz, 1H), 6.73 (s, 1H), 7.28–7.34 (m, 1H), 7.41 (d, J = 1.72 Hz, 1H), 7.51 (td, J = 8.32, 2.92 Hz, 1H), 7.60 (d, J = 8.23 Hz, 1H), 7.72 (s, 2H), 7.86 (dd, J = 8.92, 4.46 Hz, 1H); ^{13}C NMR (500 MHz, CDCl$_3$, 25 °C) δ ppm 21.06, 26.35, 37.89, 102.17, 122.08, 122.12, 123.74, 123.89, 124.28, 129.68, 131.03, 131.33, 134.78, 135.64, 138.72, 138.91, 139.07, 142.92, 142.96, 158.55, 160.62, 162.63, 167.81, 168.49.

5.2.30. N-Ethyl-N-{2-[5-(5-fluoropyridin-2-yl)-1,2-oxazol-3-yl]ethyl}-5-methyl-2-(2H-1,2,3-triazol-2-yl)benzamide (16)

60% NaH (0.011 g, 0.24 mmol) was added to a solution of compound 15 (0.080 g, 0.20 mmol) in DMF (0.68 mL), followed by stirring at room temperature for 1 h. EtI (0.018 mL, 0.22 mmol) was dropwise added to the reaction solution, followed by stirring at room temperature for 3 h. Water was added to the reaction solution, followed by extraction with EtOAc. The organic layer was washed with water and brine and was dried with Na$_2$SO$_4$. The desiccant was then removed by filtration, and the solvent was distilled off under reduced pressure. The resulting residue was purified by column chromatography (15–100% EtOAc in hexanes). The resulting solid was washed with hexane/EtOAc with stirring, followed by filtration to give the title compound 16 as a colorless powder (0.060 g, 70%). HRMS calcd for C$_{22}$H$_{21}$FN$_6$O$_2$ [M+H]$^+$ 421.1783, found 421.1777. LC–MS t = 1.05 min, [M+H]$^+$ = 421. Please see the Supplementary data for pictures of 500 MHz ^{1}H and ^{13}C NMR spectra in acetone-d_6 at 25 °C.

5.2.31. 2-{2-[3-(5-Fluoropyridin-2-yl)-1,2-oxazol-5-yl]ethyl}-1H-isoindole-1,3(2H)-dione (18)

Sodium acetate (0.32 g, 3.92 mmol) and hydroxylamine hydrochloride (0.27 g, 3.92 mmol) were added to a solution of

5-fluoropyridine-2-carbaldehyde (0.35 g, 2.80 mmol) in EtOH (10 mL) and H$_2$O (1 mL) under ice cooling. The mixture was warmed to room temperature, followed by stirring for 15 h. An aqueous NaHCO$_3$ solution was added to the reaction solution, followed by extraction with EtOAc. The organic layer was washed with brine and was dried over MgSO$_4$. The desiccant was then removed by filtration, and the solvent was distilled off under reduced pressure to give 1-(5-fluoropyridin-2-yl)-N-hydroxymethanimine as a pale yellow powder (0.27 g, 69%).

N-Chlorosuccinimide (0.28 g, 2.12 mmol) was added to a solution of 1-(5-fluoropyridin-2-yl)-N-hydroxymethanimine (0.27 g, 1.93 mmol) in DMF (5 mL) in an ice bath. The mixture was warmed to room temperature, followed by stirring for 16 h. Water was added to the reaction solution, followed by extraction with EtOAc. The organic layer was washed with brine and was dried with MgSO$_4$. The desiccant was then removed by filtration, and the solvent was distilled off under reduced pressure. The residue was dissolved in THF (5 mL), and a solution of 2-(but-3-yn-1-yl)-1H-isoindole-1,3(2H)-dione (0.58 g, 2.92 mmol) in THF (5 mL) was dropwise added to the solution in an ice bath. TEA (0.30 mL, 2.92 mmol) was further dropwise added thereto. The mixture was warmed to room temperature, followed by stirring for 3 days. Water was added to the reaction solution, followed by extraction with EtOAc. The organic layer was washed with brine and was dried with MgSO$_4$. The desiccant was then removed by filtration, and the solvent was distilled off under reduced pressure. The resulting residue was purified by column chromatography (5–50% EtOAc in hexanes) to give the title compound 18 as a pale yellow powder (0.12 g, 18% over 2 steps). HRMS calcd for C$_{18}$H$_{12}$FN$_3$O$_3$ [M+H]$^+$ 338.0935, found 338.0932. LC–MS t = 1.02 min, [M+H]$^+$ = 338.

^{1}H NMR (500 MHz, CDCl$_3$, 25 °C) δ ppm 3.25 (t, J = 7.03 Hz, 2H), 4.09 (t, J = 7.20 Hz, 2H), 6.72 (s, 1H), 7.44–7.51 (m, 1H), 7.66–7.75 (m, 2H), 7.85 (dd, J = 5.49, 3.09 Hz, 2H), 8.05 (dd, J = 8.58, 4.46 Hz, 1H), 8.49 (d, J = 2.74 Hz, 1H); ^{13}C NMR (500 MHz, CDCl$_3$, 25 °C) δ ppm 26.07, 35.84, 101.02, 122.83, 122.86, 123.55, 123.67, 123.82, 132.01, 134.22, 137.97, 138.16, 144.89, 144.92, 158.85, 160.91, 162.49, 168.01, 170.36

5.2.32. 2-[3-(5-Fluoropyridin-2-yl)-1,2-oxazol-5-yl]ethanamine (19)

Hydrazine monohydrate (0.035 mL, 0.71 mmol) was dropwise added to a solution of 2-{2-[3-(5-fluoropyridin-2-yl)-1,2-oxazol-5-yl]ethyl}-1H-isoindole-1,3(2H)-dione (0.12 g, 0.36 mmol) in EtOH (5 mL), followed by stirring at 90 °C for 2 h. After cooling at room temperature, the precipitated solid was removed by filtration. The filtrate was concentrated under reduced pressure. The resulting residue was purified by column chromatography (20–100% EtOAc in hexanes) to give the title compound 19 as a pale yellow powder (0.053 g, 72%). HRMS calcd for C$_{10}$H$_{10}$FN$_3$O [M+H]$^+$ 208.0881, found 208.0892. LC–MS t = 0.25 min, [M+H]$^+$ = 208.

^{1}H NMR (500 MHz, CDCl$_3$, 25 °C) δ ppm 2.93–3.01 (m, 2H), 3.09–3.14 (m, 2H), 6.67 (s, 1H), 7.49 (td, J = 8.32, 2.92 Hz, 1H), 8.07 (dd, J = 8.92, 4.46 Hz, 1H), 8.51 (d, J = 2.74 Hz, 1H); ^{13}C NMR (500 MHz, CDCl$_3$, 25 °C) δ ppm 31.26, 40.29, 100.56, 122.83, 123.76, 123.92, 137.98, 138.18, 145.04, 145.08, 158.85, 160.91, 162.48, 172.46.

5.2.33. N-{2-[3-(5-Fluoropyridin-2-yl)-1,2-oxazol-5-yl]ethyl}-5-methyl-2-(2H-1,2,3-triazol-2-yl)benzamide (20)

HATU (0.090 g, 0.24 mmol) was added to a solution of 2-[3-(5-fluoropyridin-2-yl)-1,2-oxazol-5-yl]ethanamine (0.053 g, 0.16 mmol), 5-methyl-2-(2H-1,2,3-triazol-2-yl)benzoic acid (0.038 g, 0.19 mmol) and DIPEA (0.082 mL, 0.47 mmol) in DMF (5 mL), followed by stirring at room temperature for 16 h. An aqueous NaHCO$_3$ solution was added to the reaction solution, followed by extraction with EtOAc. The organic layer was washed with

brine and was dried over MgSO$_4$. The desiccant was then removed by filtration, and the solvent was distilled off under reduced pressure. The resulting residue was purified by column chromatography (20–80% EtOAc in hexanes) to give the title compound **20** as a colorless powder (0.060 g, 97%). HRMS calcd for C$_{20}$H$_{17}$FN$_6$O$_2$ [M+H]$^+$ 393.1470, found 393.1485. LC–MS t = 0.90 min, [M+H]$^+$ = 393.

^{1}H NMR (500 MHz, CDCl$_3$, 25 °C) δ ppm 2.41 (s, 3H), 3.09 (t, J = 6.52 Hz, 2H), 3.73 (q, J = 6.40 Hz, 2H), 6.11 (br s, 1H), 6.65 (s, 1H), 7.33 (dd, J = 8.23, 2.06 Hz, 1H), 7.42 (d, J = 1.72 Hz, 1H), 7.49 (td, J = 8.40, 3.09 Hz, 1H), 7.61 (d, J = 8.23 Hz, 1H), 7.76 (s, 2H), 8.05 (dd, J = 8.58, 4.46 Hz, 1H), 8.50 (d, J = 2.74 Hz, 1H); ^{13}C NMR (500 MHz, CDCl$_3$, 25 °C) δ ppm 21.06, 26.88, 37.85, 100.83, 122.78, 122.82, 123.77, 123.92, 124.43, 129.72, 130.80, 131.49, 134.77, 135.75, 138.06, 138.25, 139.18, 144.88, 158.87, 160.94, 162.53, 167.89, 171.53.

5.2.34. *N*-Ethyl-*N*-{2-[3-(5-fluoropyridin-2-yl)-1,2-oxazol-5-yl]ethyl}-5-methyl-2-(2*H*-1,2,3-triazol-2-yl)benzamide (21)

The title compound **21** was prepared according to the procedure described for compound **16** from *N*-{2-[3-(5-Fluoropyridin-2-yl)-1,2-oxazol-5-yl]ethyl}-5-methyl-2-(2*H*-1,2,3-triazol-2-yl)benzamide as a colorless powder (0.032 g, 75%). HRMS calcd for C$_{22}$H$_{21}$FN$_6$O$_2$ [M+H]$^+$ 421.1783, found 421.1773. LC–MS t = 1.06 min, [M+H]$^+$ = 421. Please see the Supplementary data for pictures of 500 MHz ^{1}H and ^{13}C NMR spectra in acetone-d_6 at 25 °C.

5.2.35. *tert*-Butyl {2-[3-(5-fluoropyridin-2-yl)-1*H*-pyrazol-1-yl]ethyl}carbamate (23)

tert-Butyl *N*-(2-bromoethyl)carbamate (1.00 g, 4.49 mmol) and Cs$_2$CO$_3$ (1.83 g, 5.61 mmol) were added to a solution of 5-fluoro-2-(1*H*-pyrazol-3-yl)pyridine (0.61 g, 3.74 mmol) in DMF (10 mL), and the mixture was stirred at 80 °C for 4 h. After standing until cooled to room temperature, the reaction mixture was added to water, followed by extraction with EtOAc. The extracted organic layer was washed with brine and was dried over MgSO$_4$. Then, the desiccant was filtered off, and the solvent was distilled off under reduced pressure. The obtained residue was purified by column chromatography (20–80% EtOAc in hexanes) to obtain the title compound **23** as a colorless powder (0.55 g, 48%). HRMS calcd for C$_{15}$H$_{19}$FN$_4$O$_2$ [M+H]$^+$ 307.1565, found 307.1568. LC–MS t = 0.92 min, [M+H]$^+$ = 307.

^{1}H NMR (500 MHz, CDCl$_3$, 25 °C) δ ppm 1.42 (s, 9H), 3.61 (q, J = 5.49 Hz, 2H), 4.28 (t, J = 5.49 Hz, 2H), 6.81 (d, J = 2.06 Hz, 1H), 7.39–7.46 (m, 2H), 7.91 (dd, J = 8.58, 4.46 Hz, 1H), 8.46 (d, J = 2.74 Hz, 1H); ^{13}C NMR (500 MHz, CDCl$_3$, 25 °C) δ ppm 28.42, 40.87, 51.91, 79.81, 104.30, 121.05, 123.48, 123.63, 131.80, 137.38, 137.58, 148.70, 148.73, 151.52, 155.96, 157.88, 159.92.

5.2.36. 2-[3-(5-Fluoropyridin-2-yl)-1*H*-pyrazol-l-yl]ethanamine dihydrochloride (24)

A 4 mol/L HCl-EtOAc solution (5 mL) was added to a solution of *tert*-butyl {2-[3-(5-fluoropyridin-2-yl)-1*H*-pyrazol-1-yl]ethyl}carbamate (0.30 g, 0.98 mmol) in EtOAc (5 mL), and the mixture was stirred at room temperature for 15 h. The deposited solid was then collected by filtration. The obtained solid was dried by heating under reduced pressure to obtain the title compound **24** as a colorless powder (0.27 g, 100%). HRMS calcd for C$_{10}$H$_{11}$FN$_4$ [M+H]$^+$ 207.1041, found 207.1034. LC–MS t = 0.25 min, [M+H]$^+$ = 207.

^{1}H NMR (500 MHz, CDCl$_3$, 25 °C) δ ppm 3.01–3.48 (m, 2H), 4.44 (t, J = 6.17 Hz, 2H), 6.80 (d, J = 2.06 Hz, 1H), 7.77 (td, J = 8.75, 3.09 Hz, 1H), 7.88 (d, J = 2.40 Hz, 1H), 8.02 (dd, J = 8.75, 4.63 Hz, 1H), 8.55 (d, J = 2.74 Hz, 1H); ^{13}C NMR (500 MHz, CDCl$_3$, 25 °C) δ

ppm 39.21, 49.14, 104.76, 121.55, 121.59, 124.73, 124.88, 133.39, 137.30, 137.49, 148.75, 150.94, 158.00, 160.02.

5.2.37. *N*-{2-[4-(5-Fluoropyridin-2-yl)-1*H*-pyrazol-1-yl]ethyl}-5-methyl-2-(2*H*-1,2,3-triazol-2-yl)benzamide (25)

HATU (0.061 g, 0.16 mmol) was added to a solution of 2-[3-(5-fluoropyridin-2-yl)-1*H*-pyrazol-l-yl]ethanamine dihydrochloride (0.030 g, 0.11 mmol), 5-methyl-2-(2*H*-1,2,3-triazol-2-yl)benzoic acid (0.026 g, 0.13 mmol) and DIPEA (0.094 mL, 0.54 mmol) in DMF (5 mL), followed by stirring at room temperature for 3 h. An aqueous NaHCO$_3$ solution was added to the reaction solution, followed by extraction with EtOAc. The organic layer was washed with brine and was dried over MgSO$_4$. The desiccant was then removed by filtration, and the solvent was distilled off under reduced pressure. The resulting residue was purified by column chromatography (20–80% EtOAc in hexanes). The resulting solid was washed with Et$_2$O with stirring, followed by filtration to give the title compound **25** as a colorless powder (0.021 g, 50%). HRMS calcd for C$_{20}$H$_{18}$FN$_7$O [M+H]$^+$ 392.1630, found 392.1612. LC–MS t = 0.82 min, [M+H]$^+$ = 392.

^{1}H NMR (500 MHz, acetone-d_6, 25 °C) δ ppm 2.35 (s, 4H), 3.74 (q, J = 6.17 Hz, 3H), 4.37 (t, J = 6.00 Hz, 4H), 6.77 (d, J = 2.40 Hz, 2H), 7.23–7.45 (m, 3H), 7.60 (td, J = 8.66, 2.92 Hz, 1H), 7.64 (d, J = 8.23 Hz, 1H), 7.78 (d, J = 2.40 Hz, 1H), 7.88 (s, 2H), 8.01–8.05 (m, 1H); ^{13}C NMR (500 MHz, acetone-d_6, 25 °C) δ ppm 20.01, 40.07, 50.97, 103.81, 120.57, 123.23, 123.38, 123.71, 129.31, 130.70, 131.80, 131.99, 135.30, 135.61, 136.77, 136.96, 138.39, 149.45, 151.08, 157.88, 159.90, 167.32.

5.2.38. *N*-{2-[3-(5-Fluoropyridin-2-yl)-1*H*-pyrazol-1-yl]ethyl}-*N*,5-dimethyl-2-(2*H*-1,2,3-triazol-2-yl)benzamide (26a)

The title compound **26a** was prepared according to the procedure described for compound **16** from *N*-{2-[4-(5-fluoropyridin-2-yl)-1*H*-pyrazol-1-yl]ethyl}-5-methyl-2-(2*H*-1,2,3-triazol-2-yl)benzamide and MeI which was used instead of EtI as colorless powder (0.34 g, 100%). HRMS calcd for C$_{21}$H$_{20}$FN$_7$O [M+H]$^+$ 406.1786, found 406.1775. LC–MS t = 0.93 min, [M+H]$^+$ = 406. Please see the Supplementary data for pictures of 500 MHz ^{1}H and ^{13}C NMR spectra in acetone-d_6 at 25 °C.

5.2.39. *N*-{2-[4-(5-Fluoropyridin-2-yl)-1*H*-pyrazol-1-yl]ethyl}-5-methyl-*N*-(propan-2-yl)-2-(2*H*-1,2,3-triazol-2-yl)benzamide (26b)

The title compound **26b** was prepared according to the procedure described for compound **16** from *N*-{2-[4-(5-fluoro-pyridin-2-yl)-1*H*-pyrazol-1-yl]ethyl}-5-methyl-2-(2*H*-1,2,3-triazol-2-yl)benzamide and *i*PrI which was used instead of EtI as colorless powder (0.052 g, 12%). HRMS calcd for C$_{23}$H$_{24}$FN$_7$O [M+H]$^+$ 434.2099, found 434.2099. LC–MS t = 1.10 min, [M+H]$^+$ = 434. Please see the Supplementary data for pictures of 500 MHz ^{1}H and ^{13}C NMR spectra in acetone-d_6 at 25 °C.

Supplementary data

Supplementary data (reproduction of the ^{1}H and ^{13}C NMR spectra for key compounds) associated with this article can be found, in the online version, at http://dx.doi.org/10.1016/j.bmc.2015.01.044.

References and notes

1. Sakurai, T.; Amemiya, A.; Ishii, M.; Matsuzaki, I.; Chemelli, R. M.; Tanaka, H.; Williams, S. C.; Richardson, J. A.; Kozlowski, G. P.; Wilson, S.; Arch, J. R.; Buckingham, R. E.; Haynes, A. C.; Carr, S. A.; Annan, R. S.; McNulty, D. E.; Liu, W. S.; Terrett, J. A.; Elshbagy, N. A.; Bergsma, D. J.; Yanagisawa, M. *Cell* **1998**, *92*, 573.
2. De Lecea, L.; Kilduff, T. S.; Peyron, C.; Gao, X.; Foye, P. E.; Danielson, P. E.; Fukuhara, C.; Battenberg, E. L.; Gautvik, V. T.; Bartlett, F. S., 2nd; Frankel, W. N.; van den Pol, A. N.; Bloom, F. E.; Gautvik, K. M.; Sutcliffe, J. G. *Proc. Natl. Acad. Sci. U.S.A.* **1998**, *95*, 322.
3. Zhu, Y.; Miwa, Y.; Yamanaka, A.; Yada, T.; Shibahara, M.; Abe, Y.; Sakurai, T.; Goto, K. *J. Pharmacol. Sci.* **2003**, *92*, 259.
4. Tsujino, N.; Sakurai, T. *Pharmacol. Rev.* **2009**, *61*, 162.
5. Hoyer, D.; Jacobson, L. H. *Neuropeptides* **2013**, *47*, 477.
6. Lin, L.; Faraco, J.; Li, R.; Kadotani, H.; Rogers, W.; Lin, X.; Qiu, X.; De Jong, P. J.; Nishino, S.; Mignot, E. *Cell* **1999**, *98*, 365.
7. Gotter, A. L.; Winrow, C. J.; Brunner, J.; Garson, S. L.; Fox, S. V.; Binns, J.; Harrell, C. M.; Cui, D.; Yee, K. L.; Stiteler, M.; Stevens, J.; Savitz, A.; Tannenbaum, P. L.; Tye, S. J.; McDonald, T.; Yao, L.; Kuduk, S. D.; Uslaner, J.; Coleman, P. J.; Renger, J. J. *BMC Neurosci.* **2013**, *14*, 90.
8. Scammell, T. E.; Winrow, C. J. *Annu. Rev. Pharmacol. Toxicol.* **2011**, *51*, 243.
9. Winrow, C. J.; Renger, J. J. *Br. J. Pharmacol.* **2014**, *171*, 283.
10. Michelson, D.; Snyder, E.; Paradis, E.; Chengan-Liu, M.; Snavely, D. B.; Hutzelmann, J.; Walsh, J. K.; Krystal, A. D.; Benca, R. M.; Cohn, M.; Lines, C.; Roth, T.; Herring, W. J. *Lancet Neurol.* **2014**, *13*, 461.
11. Sun, H.; Kennedy, W. P.; Wilbraham, D.; Lewis, N.; Calder, N.; Li, X.; Ma, J.; Yee, K. L.; Ermlich, S.; Mangin, E.; Lines, C.; Rosen, L.; Chodakewitz, J.; Murphy, G. M. *Sleep* **2013**, *36*, 259.
12. Bettica, P.; Nucci, G.; Pyke, C.; Squassante, L.; Zamuner, S.; Ratti, E.; Gomeni, R.; Alexander, R. *J. Psychopharmacol.* **2012**, *26*, 1058.
13. Bettica, P.; Squassante, L.; Groeger, J. A.; Gennery, B.; Winsky-Sommerer, R.; Dijk, D. J. *Neuropsychopharmacology* **2012**, *37*, 1224.
14. Bettica, P.; Squassante, L.; Zamuner, S.; Nucci, G.; Danker-Hopfe, Hatti; Ratti, E. *Sleep* **2012**, *35*, 1097.
15. Cox, C. D.; McGaughey, G. B.; Bogusky, M. J.; Whitman, D. B.; Ball, R. G.; Winrow, C. J.; Renger, J. J.; Coleman, P. J. *Bioorg. Med. Chem. Lett.* **2009**, *19*, 2997.
16. Molecular Operating Environment (MOE), 2013.08; Chemical Computing Group Inc., 1010 Sherbooke St. West, Suite #910, Montreal, QC, Canada, H3A 2R7, 2013.
17. Accelrys Software Inc., Discovery Studio Modeling Environment, Release 4.0 San Diego: Accelrys Software Inc., 2013.
18. Ito, S.; Hirata, Y.; Satoh, A.; Nagatomi, Y.; Suzuki, G.; Kimura, T.; Satow, A.; Maehara, S.; Hikichi, H.; Hata, M.; Ohta, H.; Kawamoto, H. *Bioorg. Med. Chem. Lett.* **2009**, *19*, 5310.
19. Waring, M. J. *Expert Opin. Drug. Discov.* **2010**, *5*, 235.
20. Hosea, N. A.; Collard, W. T.; Cole, S.; Mauer, T. S.; Fang, R. X.; Jones, H.; Kakar, S. M.; Nakai, Y.; Smith, B. J.; Webster, R.; Beaumont, K. *J. Clin. Pharmacol.* **2009**, *49*, 513.